

SYNTHESIS OF GOLD NANOWIRES WITH HIGH ASPECT RATIO AND  
MORPHOLOGICAL PURITY

A THESIS SUBMITTED TO  
THE GRADUATE SCHOOL OF NATURAL AND APPLIED SCIENCES  
OF  
MIDDLE EAST TECHNICAL UNIVERSITY

BY

ELÇİN DERTLİ

IN PARTIAL FULFILLMENT OF THE REQUIREMENT  
FOR  
THE DEGREE OF MASTER OF SCIENCE  
IN  
MICRO AND NANOTECHNOLOGY

SEPTEMBER 2012

Approval of the thesis:

**SYNTHESIS OF GOLD NANOWIRES WITH HIGH ASPECT RATIO AND MORPHOLOGICAL PURITY**

submitted by **ELÇİN DERTLİ** in partial fulfillment of the requirements for the degree of **Master of Science in Micro and Nanotechnology Department, Middle East Technical University** by,

Prof. Dr. Canan ÖZGEN \_\_\_\_\_  
Dean, Graduate School of **Natural and Applied Sciences**

Prof. Dr. Mürvet VOLKAN \_\_\_\_\_  
Head of Department, **Micro and Nanotechnology**

Assoc. Prof Dr. Emren NALBANT ESENTÜRK \_\_\_\_\_  
Supervisor, **Chemistry Dept., METU**

Assoc. Prof. Dr. Hüsnü Emrah ÜNALAN \_\_\_\_\_  
Co-Supervisor, **Metallurgical and Materials Eng Dept., METU**

**Examining Committee Members:**

Prof. Dr. Hacer Ceyhan KAYRAN \_\_\_\_\_  
Chemistry Dept., METU

Assist. Prof. Dr. Emren NALBANT ESENTÜRK \_\_\_\_\_  
Chemistry Dept., METU

Assist. Prof. Dr. Hüsnü Emrah ÜNALAN \_\_\_\_\_  
Metallurgical and Materials Eng. Dept., METU

Assoc Prof. Dr. Caner DURUCAN \_\_\_\_\_  
Metallurgical and Materials Eng Dept., METU

Assoc. Prof. Dr. Ali ÇIRPAN \_\_\_\_\_  
Chemistry Dept., METU

Date: 03/09/2012

**I hereby declare that all information in this document has been obtained and presented in accordance with academic rules and ethical conduct. I also declare that, as required by these rules and conduct, I have fully cited and referenced all material and results that are not original to this work.**

Name, Last name: ELÇİN DERTLİ

Signature:

## **ABSTRACT**

### **SYNTHESIS OF GOLD NANOWIRES WITH HIGH ASPECT RATIO AND MORPHOLOGICAL PURITY**

DERTLİ, Elçin

M.S., Department of Micro and Nanotechnology

Supervisor: Assoc. Prof. Dr. Emren NALBANT ESENTÜRK

Co-Supervisor: Assoc. Prof. Dr. Hüsnü Emrah ÜNALAN

September 2012, 59 pages

Metal nanoparticles have unique optical, electrical, catalytic and mechanical properties, which lead them to various applications in nanotechnology. In particular, noble metal nanowires are attracting growing attention due to their potential applications such as in opto-electronic devices and transparent conductive contacts (TCCs). There are two general approaches to synthesize nanowires: template-assisted and solution phase methods. However, these synthesis approaches have various disadvantages. For example, removal of the template to ensure the purity of the synthesized nanowires is the major problem. In solution methods like the widely used “seed mediated growth method”, nanowires are synthesized in low yield with the significant amount of by-products and requirement of purification is a major problem for further applications. Among all solution based methods, hydrothermal process is a very promising way of preparing gold (Au) nanowires in high yield and structural purity.

In this thesis, hydrothermal process was modified to synthesize high aspect ratio Au nanowires with high morphological purity. Parametric study was performed to examine the effect of surfactant concentration, reaction time and temperature on the quality of products. The optimum conditions were determined for two different surfactant molecules (hexamethylenetetramine (HMTA) and ethylenediaminetetraacetic acid ( $\text{Na}_2\text{-EDTA}$ )). Characterization of the products was done by detailed analysis via scanning electron microscopy (SEM), transmission electron microscopy (TEM), energy-dispersive spectroscopy (EDS), X-Ray diffraction (XRD) and X-Ray photoelectron spectroscopy (XPS). The analyses demonstrated that the Au nanowires synthesized at optimum conditions have high aspect ratio (diameters 50-110 nm range and lengths in micrometer range) and high structural purity.

Keywords: High aspect ratio, Au nanowire, hydrothermal method

## ÖZ

### YÜKSEK EN/BOY ORANINDA VE YAPISAL SAFLIKTAKİ ALTIN NANOTELLERİN SENTEZİ

DERTLİ, Elçin

Yüksek Lisans, Mikro ve Nanoteknoloji Bölümü

Tez Yöneticisi: Yrd. Doç. Dr. Emren NALBANT ESENTÜRK

Ortak Tez Yöneticisi: Yrd. Doç. Dr. Hüsnü Emrah ÜNALAN

Eylül 2012, 59 sayfa

Metal nano parçacıkların nanoteknolojide birçok uygulama alanında kullanılmasına sebep olan kendilerine özgü optik, elektronik, katalitik ve mekanik özellikleri vardır. Opto-elektronik cihazlar ve şeffaf iletken elektrotlar gibi potansiyel uygulama alanlarından dolayı, özellikle soy metal nanoteller ilgi odağı haline gelmişlerdir. Nanotellerin sentezi için iki genel yaklaşım vardır: kalıp-yardımlı ve solüsyon fazlı yöntemler. Ancak bu yöntemler birçok dezavantaja sahiptirler. Örneğin, sentezlenen nanotellerin saflığını sağlamak amacıyla kalıbın uzaklaştırılması büyük problemdir. Solüsyon metotlarından en çok kullanılan “Çekirdek aracılığı ile büyüme yöntemi” gibi yöntemlerde, nanotellerin çok düşük verimle oluşmasıyla birlikte kayda değer oranda yan ürün elde edilmesi ve saflaştırma zorunlulukları daha sonraki uygulamalar için büyük problemlerdir. Bütün solüsyon temelli metotların içerisinde, hidrotermal süreç altın nanotellerin yüksek verimde ve yapısal saflıkta elde edilmelerinde umut verici bir yöntemdir.

Bu tez çalışmasında, hidrotermal metot yüksek en/boy oranı ve yüksek yapısal saflığa sahip altın nanotellerin sentezi için modifiye edilmiştir. Yüzey aktif madde konsantrasyonu, reaksiyon zamanı ve sıcaklığın ürünün kalitesine etkisini araştırmak için parametrik çalışma yapılmıştır. İki farklı yüzey aktif madde (hekzametilentetramin (HMTA) ve etilendiamintetraasetik asit ( $\text{Na}_2\text{-EDTA}$ )) için uygun koşullar belirlenmiştir. Ürünlerin detaylı karakterizasyon çalışmaları taramalı elektron mikroskobu (SEM), tarayıcı elektron mikroskobu (TEM), enerji saçılım spektroskopu (EDS), X-ışını kırınım yöntemi (XRD) ve X-ışını fotoelektron spektroskopisi (XPS) aracılığı ile yapılmıştır. Analiz sonuçları uygun koşullarda altın nanotellerin yüksek en/boy oranında (çapları 50-110 nm aralığında ve boyları mikrometre boyutunda/seviyesinde) ve yüksek yapısal saflıkta elde edildiklerini göstermektedir.

Anahtar Kelimeler: Yüksek en/boy oranı, altın nanotel, hidrotermal yöntem

***To My Family...***

## ACKNOWLEDGMENTS

I would like to express my sincere gratitude to my supervisor Assoc. Prof. Dr. Emren Nalbant Esentürk, for providing me with amazing support and encouragement during my research. I am honored to have her as my mentor and I am forever grateful for her time, energy, wisdom, insight, and friendship. In addition, I would also like to express my thanks to my co-advisor, Assoc. Prof. Dr. Hüsnü Emrah Ünal, for sharing his knowledge and talents with me and for his generous donation of his time and experience.

A special word of thanks also goes to Şahin Coşkun for spending infinite hours of SEM sessions and moreover for the inspiration he provided to ensure the completion of this work. I also would like to thank Yüksel Çabuk and Emin Ünal for helping the design of experimental setup.

I am also grateful to my friend Özüm Öyküm Yurtseven for her endless help. Throughout all of the master period, she provided encouragement, sound advice, good company, and lots of good ideas and I would have been lost without her.

I owe my deepest gratitude to my lab-mates Duygu Kozanoğlu, Zhanar Sholonbayeva, Esra Ogün, Doruk Ergöçmen, Betül Çağla Arca and Asude Çetin. I will never forget the awesome time we have had together and I feel very lucky to get to know such great people.

I also thank all of my great friend Zeynep Kırışak, Kübra Eren, Özgür Kazar, Ertuğ Kılavuz, Efe Arslan, Gökben Ö for their infinite support, patience and kindness.

Finally, I thank my father, Mehmet Dertli, my mother, Solmaz Dertli, and my sister, Evrim Çiçek and also Kuzey Mert Çiçek and Gökhan Çiçek for their

endless love and support in every moment of my life. Without my family; this thesis would not have been possible.

## TABLE OF CONTENTS

ABSTRACT.....	iv
ÖZ.....	vi
ACKNOWLEDGEMENT .....	vii
TABLE OF CONTENTS.....	x
LIST OF FIGURES .....	xii
CHAPTERS	
1. INTRODUCTION.....	1
2. GOLD NANOWIRE SYNTHESIS METHODS.....	- 4 -
2.1 Introduction .....	- 4 -
2.2 General Aspects of Nanowires .....	- 5 -
2.3 Synthesis of Au Nanowires .....	- 10 -
2.3.1 Top-Down Gold Nanowire Synthesis Method.....	- 11 -
2.4 Comparison of Modified Hydrothermal Process with the Conventional Methods.....	- 27 -
3. EXPERIMENTAL .....	- 28 -
3.1 Materials .....	- 28 -
3.2 Methods .....	- 28 -
3.3 Characterization.....	- 30 -
4. RESULTS AND DISCUSSION.....	- 31 -
4.1 Introduction .....	- 31 -

4.2 Deposition of Au Ions onto Resin and Their Reduction Process .....	- 32 -
4.3 Determination of the Modified Hydrothermal Process Parameters.....	- 38 -
4.3.1 Effect of Surfactant.....	- 38 -
4.3.2 Effect of Temperature.....	- 44 -
4.3.3 Effect of Reaction Time .....	- 49 -
5. CONCLUSIONS.....	- 53 -
REFERENCES .....	- 54 -

## LIST OF FIGURES

### FIGURES

- Figure 1** Calculated surface to bulk atom ratios (for spherical Fe). ..... - 5 -
- Figure 2** Dimensionality classification of nanostructures..... - 6 -
- Figure 3** Different shapes of nanostructured materials..... - 6 -
- Figure 4** Applications of nanowires (a) Lithium batteries, (b) Solar cells, (c) Biological sensors, (d) Light emitting diodes, (e) Field effect transistors (FETs), (f) Memory storage..... - 8 -
- Figure 5** Au nanowire applications: (a) Gas sensor, (b) Tissue-engineered cardiac patches, (c) Transparent conducting contacts, (d) Electrodes for biosensing..... - 9 -
- Figure 6** Au nanowire synthesis methods. .... - 11 -
- Figure 7** SEM images of the SERS-active substrates: array of Au nanowires with variable length,  $L$  (A:  $L = 420$  nm, B:  $L = 620$  nm, C:  $L = 720$  nm, D:  $L = 1$   $\mu$ m), 50 nm height, 60 nm width ( $l$ ). The inter-particle spacings are constant for all arrays and are fixed to 150 nm (PPX and PPY). Scale bars : 2  $\mu$ m for A and 1  $\mu$ m for B, C and D. .... - 12 -
- Figure 8** Schematic illustration of the different templates used in Au nanowire synthesis through template-assisted method; (a) Anodic aluminum oxide (AAO) membrane, (b) Copolymer template and (c) Micelle soft templates..... - 14 -
- Figure 9** SEM picture of synthesized Au wires through template-assisted method..... - 15 -
- Figure 10** Schematic illustration of synthesis of Au nanowire through template assisted method modified with electrodeposition. .... - 16 -
- Figure 11** a)Scheme of synthesis of Au nanowires via step edge decoration, b)SEM image of Au nanowires..... - 17 -
- Figure 12** TEM images of Au nanowires synthesized via template assisted method..... - 18 -

<b>Figure 13</b> SEM micrographs of (a) Au nanorod arrays grown in PC membranes covering a large area with uniform size and density, (b) Au nanotubes, ascribed to possible growth propagating along the surface of pore channels, and (c) Au nanorods, attributing to uniform growth from the bottom of pore channels attached to the electrode. ....	- 19 -
<b>Figure 14</b> (a) TEM image of unsupported Au nanowires. (a) The arrows highlight the bridges between the nanowires. The inset shows select-area electron diffraction. (b) The enlarged image of ellipse portion of image.....	- 20 -
<b>Figure 15</b> Schematic illustration of synthesis of Au rod/nanowire through seed mediated method (a) SEM picture of Au nanorods (b) SEM picture of Au nanowires synthesized in acidic media.....	- 22 -
<b>Figure 16</b> Picture of Autoclave .....	- 23 -
<b>Figure 17</b> Tungsten light-bulb fitted setup.....	- 25 -
<b>Figure 18</b> Micrometer long Au nanowires.....	- 25 -
<b>Figure 19</b> SEM images of different types of nanostructures via modified hydrothermal method (a) CuS nanoplates (b) ZnO nanococoons (c) Fe <sub>3</sub> O <sub>4</sub> nanowafers (d) TiO <sub>2</sub> nanoflowers.....	- 26 -
<b>Figure 20</b> Photographs of (a) mixture of HAuCl <sub>4</sub> solution (yellow colored) with anion exchange resin (colorless beads); (b) Au ions are deposited onto anion exchange resin (color became orange) after 30 minutes of stirring; as-synthesized Au nanowires in the presence of (c) Na <sub>2</sub> -EDTA and (d) HMTA after 4 hours of heating. ....	- 29 -
<b>Figure 21</b> Schematic illustration of (a) deposition of Au ions onto anion exchange resin (b) growth process of Au nanowires though electrostatic field force and dipole-dipole interaction. ....	- 33 -
<b>Figure 22</b> Characterization of Au nanowires synthesized with HMTA (a) SEM images, (b) XRD pattern, (c) XPS spectra and (d) TEM image. Inset shows HRTEM image and SAED pattern for the nanowires. ....	- 35 -
<b>Figure 23</b> Characterization of Au nanowires synthesized with Na <sub>2</sub> -EDTA (a) SEM images, (b) XRD pattern, (c) XPS spectra and (d) TEM image. Inset shows HRTEM image and SAED pattern for the nanowires. ....	- 36 -
<b>Figure 24</b> EDS analysis of synthesized Au nanowires in the presence of (a) HMTA and (b) Na <sub>2</sub> -EDTA.....	- 37 -

**Figure 25** (a) Au micro structures synthesized with HMTA lower than optimum amount (b) Au nanowires synthesized with sufficient amount of HMTA (c) SEM image of micro structures (d) SEM image of nanowires.. - 39 -

**Figure 26** (a) Au micro structures synthesized with Na<sub>2</sub>-EDTA lower than optimum amount (b) Au nanowires synthesized with sufficient amount of Na<sub>2</sub>-EDTA (c) SEM image of micro structures (d) SEM image of nanowires. . - 40 -

**Figure 27** SEM images of Au nanostructures synthesized at different HMTA concentrations of (a) 0.03, (b) 0.05, (c) 0.1, (d) 0.3, and (e) 0.5 M. .... - 42 -

**Figure 28** SEM images of Au nanostructures synthesized at different Na<sub>2</sub>-EDTA concentration of (a) 0.01, (b) 0.03, (c) 0.1, and (d) 0.3 M. .... - 43 -

**Figure 29** Skeletal formulas of (a) Na<sub>2</sub>-EDTA (b) HMTA. .... - 44 -

**Figure 30** SEM images of Au nanowires synthesized in the presence of HMTA at different temperatures (a) 70, (b) 90, (c) 110, (d) 125 and (e) 150 °C..... - 46 -

**Figure 31** SEM images of Au nanowires synthesized in the presence of Na<sub>2</sub>-EDTA at different temperatures (a) 70, (b) 90, (c) 110, (d) 125 and (e) 150 °C. (f) Changes in nanowire diameter with reaction temperature..... - 48 -

**Figure 32** SEM images of Au nanostructures synthesized in the presence of HMTA at 110 °C for (a) 10 min, (b) 30 min, (c) 2 hours, (d) 4 hours and (e) 5 hours..... - 50 -

**Figure 33** SEM images of Au nanostructures synthesized in the presence of Na<sub>2</sub>-EDTA at 125 °C for (a) 10 min, (b) 30 min, (c) 2 hours, (d) 4 hours and (e) 5 hours..... - 52 -

# CHAPTER 1

## INTRODUCTION

Decreasing the size of materials provides them high volume fraction of the grain boundaries and interfaces so that novel mechanic, catalytic, electronic and optical characteristics are obtained compared to the bulk materials. To date, noble metals, semiconductors and magnetic materials are mostly studied by researchers. In particular, noble metal nano materials are promising candidates for future applications such as organic solar cells, light-emitting diodes, catalysis, and cancer therapy due to their size-dependent fascinating optical properties. Depending on the purpose of applications, gold (Au) nano particles can be prepared with various size and shapes such as star, sphere, cube, and wire. Due to their high surface area and quantum confinement effect, particularly Au nanowires have attracted much attention for the applications where direct electrical conduction rather than tunneling transport is preferred.

Au nanowires can be prepared with two general approaches: “top-down” and “bottom-up.” Top-down techniques such as e-beam lithography (EBL) and focused ion beam (FIB) lithography can be carried out to synthesize Au nanorods. Bottom-up techniques are more preferable than top-down techniques because of their simplicity, possibility of having control over size and shape of nanomaterials in molecular level. The most widely used bottom-

up Au nanowire fabrication method is the template-assisted method. This method requires membranes such as porous anodic alumina films, etched ion-track membranes (EITM), and mesoporous silica. Recently, biotemplates (i.e. DNA) have also been discovered for the formation of Au nanowires. Template methods can also be adapted to many different synthesis methods including electrochemical, photochemical, electroless methods. However, challenging template removal steps which may result in damaging nanowire structure and complex experimental setups are major drawbacks of template-assisted methods.

Another widely used bottom-up approach to provide Au nanowires is solution based methods. Particularly, seed mediated growth has been widely used to synthesis of Au nano rods/wires. The method involves reduction of Au salt in aqueous media in the presence of surfactant molecule which is directing the anisotropic growth of nanoparticles. It is a very facile way to synthesize Au nanowires or nanoparticles with different morphologies. However, the nanowires are formed with significant amount of by-products, therefore time consuming purification steps are required.

On the other hand, modified hydrothermal (MHT) process, which is rather new, is a very promising way to synthesize Au nanowires with gram quantities and high purity. Also, it has advantage of being affordable, simple and efficient. MHT process is based on two steps; deposition of Au ions on an anion exchange resin and reduction of Au (III) with the help of surfactant which is reducing as well as growth controlling agent at elevated temperatures and pressures. Unlike other conventional methods, the MHT process provide synthesis of Au nanowires with lengths in micrometer size ( $10\ \mu\text{m}$ ) and diameters in the range of 50 nm to 100 nm. Therefore, the Au nanowires prepared with this method have a great potential for applications

such as transparent conducting contacts, organic light emitting diodes or solar cells in nano opto-electronic devices.

## CHAPTER 2

### GOLD NANOWIRE SYNTHESIS METHODS

#### 2.1 Introduction

In the last 30 years, there has been a profound impact on the improvement in nanotechnology. Nanotechnology is defined as controlling or manipulating atomic, molecular structure of materials in nano scale and obtaining materials with novel characteristic. These novel materials can be integrated into the conventional large systems or sub-micron systems to develop innovative technologies.

Conventional materials have grain sizes ranging from microns to several millimeters and contain several billion atoms each. On the other hand, nano structured materials contain tens of atoms and small sized grains. As the grain size decreases, there is a significant increase in the volume fraction of grain boundaries or interfaces. Since the nano crystalline material contains a high density of interfaces, a substantial fraction of atoms lie in the interfaces. Therefore, higher chemical potential at the surface of nano materials is observed compared to the bulk materials (Figure 1). Moreover, increase in the volume fraction of grain boundaries in nano regime may also significantly alter properties (i.e. optical, mechanical, catalytic and electrical) of materials compared to conventional bulk materials. Also some other properties such as melting point or magnetic properties can exhibit a

significant change in nano regime due to the high number of atoms found at surface. [1]

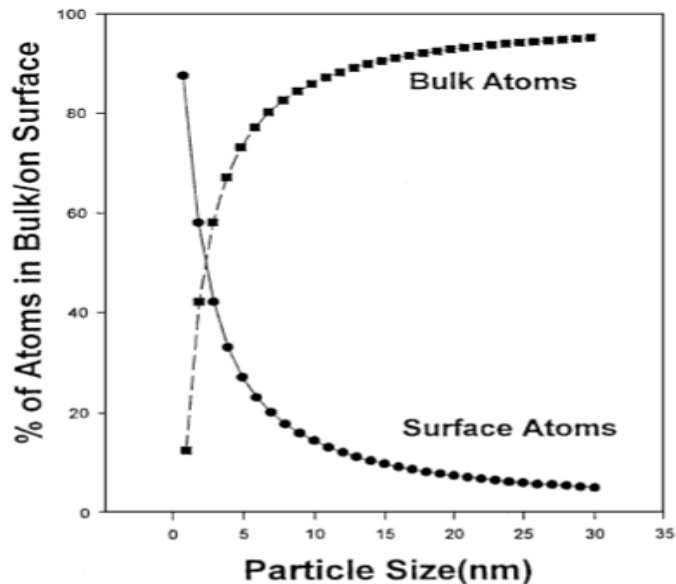


**Figure 1** Calculated surface to bulk atom ratios (for spherical Fe) [2].

## 2.2 General Aspects of Nanowires

Different synthesis methods enable the synthesis of nanostructured materials with different dimensions and morphologies. In general, nanomaterials in four different dimensions have been reported. These are zero dimensional (0-D) quantum dots, nanospheres; one dimensional (1-D) nanowires/nanotubes and quantum wires; two dimensional (2-D) thin films, layered films, quantum wells; and three dimensional (3D) nanoparticles (Figure 2). The size and shape of nano materials are very important since morphology of nano particles can make significant change on their properties (Figure 3)

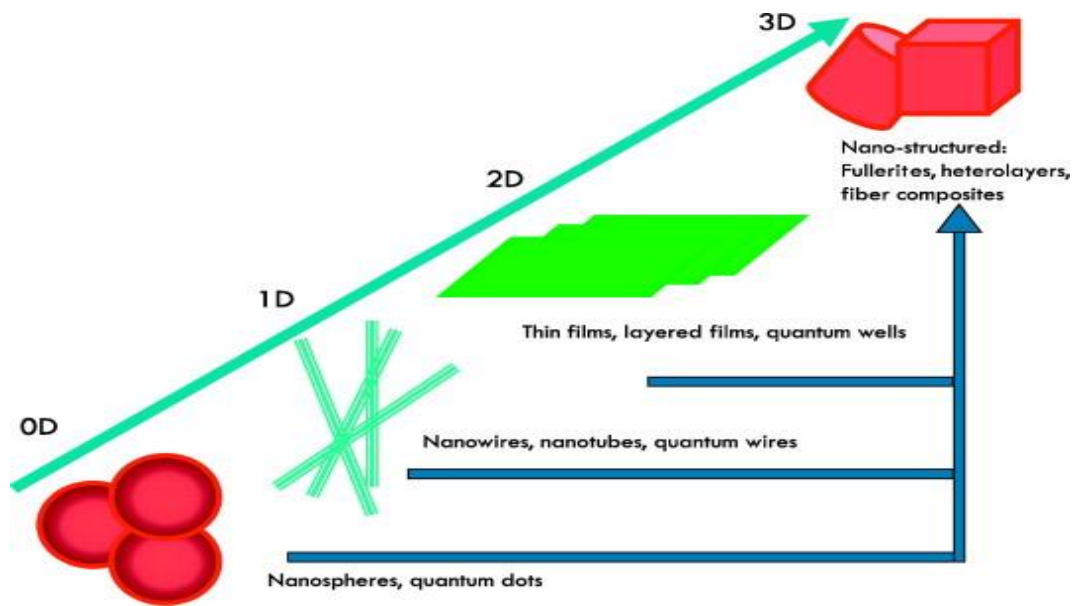


**Figure 2** Dimensionality classification of nanostructures [3].

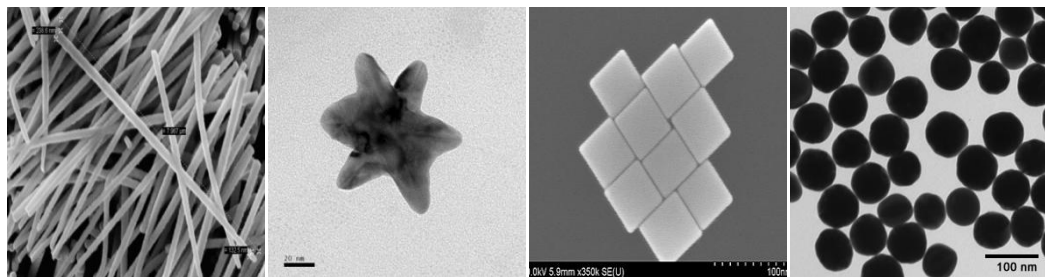


**Figure 3** Different shapes of nanostructured materials.

Nanowires can have lengths longer than 600 nm with diameter between 10-100 nm [4]. These 1D structures have two quantum-confined directions and third one is unconfined which makes them suitable for electrical conduction. Therefore they are potential transparent conducting contacts (TCCs), where electrical conduction, rather than tunneling transport, is required [5].

Nanowires made of metallic (Cu, Co, Ni, Pt, Au, Ag), semiconductor (CdS, CdTe, InP, Si, GaN) and insulator ( $\text{SiO}_2$ ,  $\text{TiO}_2$ ) materials are some of the widely studied examples up to date. For example, basic electronic devices, opto-electronic devices (i.e. junction diodes, lithium batteries) [6], light emitting diodes (LEDs) [7] and solar cells [8] can be fabricated with the help of Si and GaN nanowires [9]. Moreover, Si [10] and Ge [11] nanowires provide elimination or minimization of source-drain capacitance in bulk field effect transistors (FETs), which have been attracted great deal of attention lately. Chemical and biological sensors [12] are other interesting applications, where large surface area to volume ratio become very important. Si,  $\text{SnO}_2$ , ZnO, and  $\text{In}_2\text{O}_3$  nanowires can be given as examples for this particular application (Figure 4) [13]

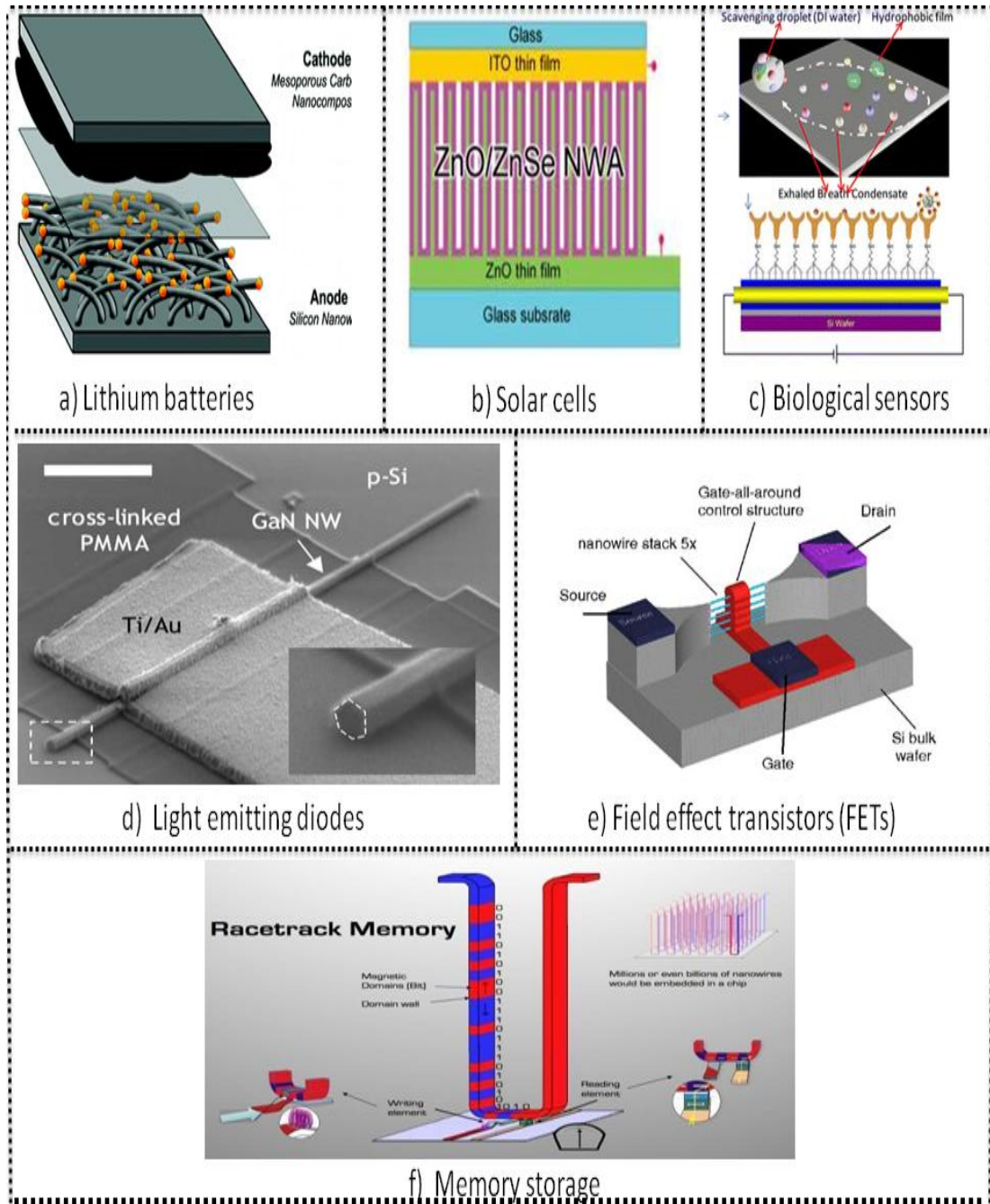


**Figure 4** Applications of nanowires (a) Lithium batteries, (b) Solar cells, (c) Biological sensors, (d) Light emitting diodes, (e) Field effect transistors (FETs), (f) Memory storage [6-8].

Among all wire structured nanomaterials, Au ones are especially interesting since they have numerous advantages which make them technologically important. Au is highly inert and resistant to many harsh chemicals such as nitric acid, sulfur based tarnishing [14]. Their high chemical and thermal stability makes Au nanowires desirable for various applications. Additionally, their biocompatible and low toxicity characteristics enable them to utilize in many biological applications [15]. Above all, their low resistivity ( $2.2 \mu\Omega \text{ cm}$ ) makes them very compatible for nano-electronic, opto-electronic devices [16] (Figure 5)

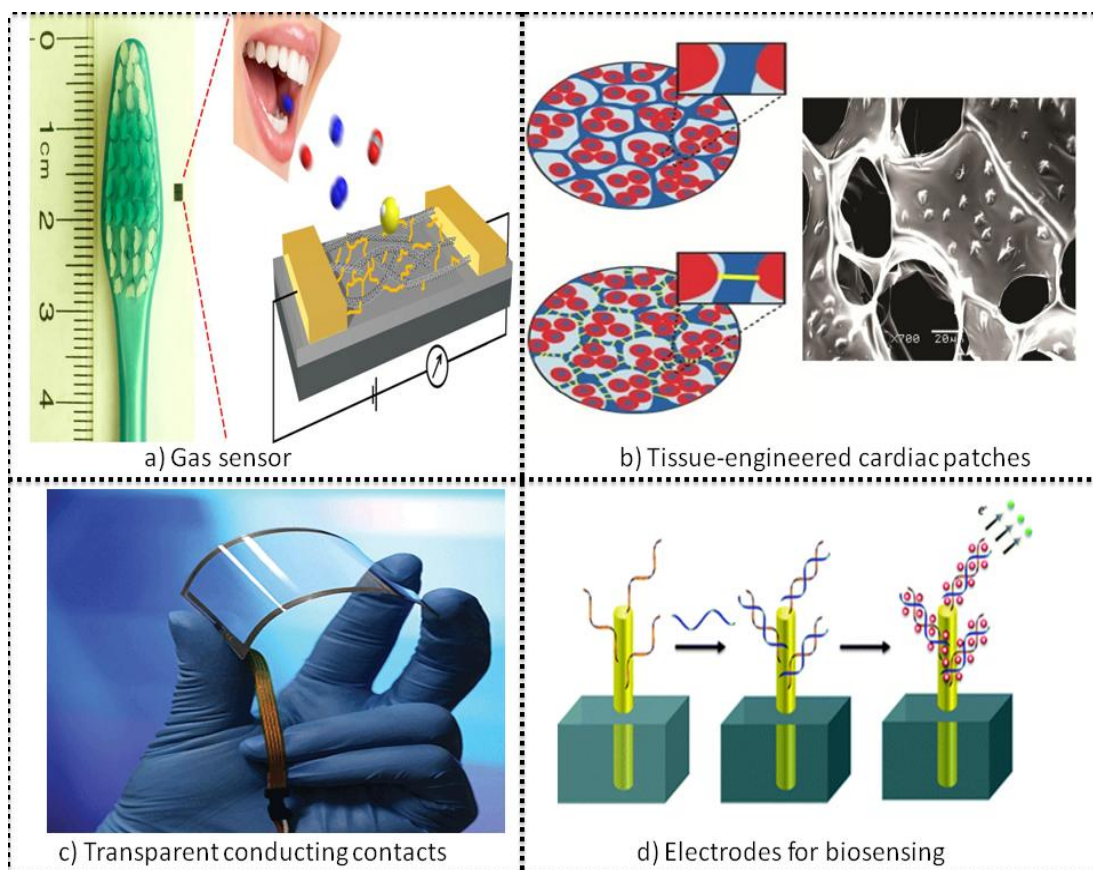


**Figure 5** Au nanowire applications: (a) Gas sensor, (b) Tissue-engineered cardiac patches, (c) Transparent conducting contacts, (d) Electrodes for biosensing [17-20].

### 2.3 Synthesis of Au Nanowires

Different kinds of fabrication methods, which are listed in Figure 6, have been reported for synthesis of Au nanowires. In general, the synthesis of Au nanowires consists of two general approaches named as “top-down” and “bottom-up”. The first one is “top-down”. Top-down method can be defined as breaking of bulk material down to structures in nano scale. E-beam lithography [21] can be given as an example of “top-down” approach to make Au nanowires. On the other hand “bottom-up” approach based on combining small components, atoms or molecules into bigger and more complex materials. The most widely used bottom-up Au nanowire fabrication method is template-assisted method which can be integrated with electrochemical, photochemical or electroless methods. Also, seed-mediated [22] and modified hydrothermal processes [23] are other examples of bottom-up techniques. Due to their simplicity, possibility of having control over size, shape & properties of nanomaterials in molecular level, bottom-up techniques are more preferred and widely used compared to top-down

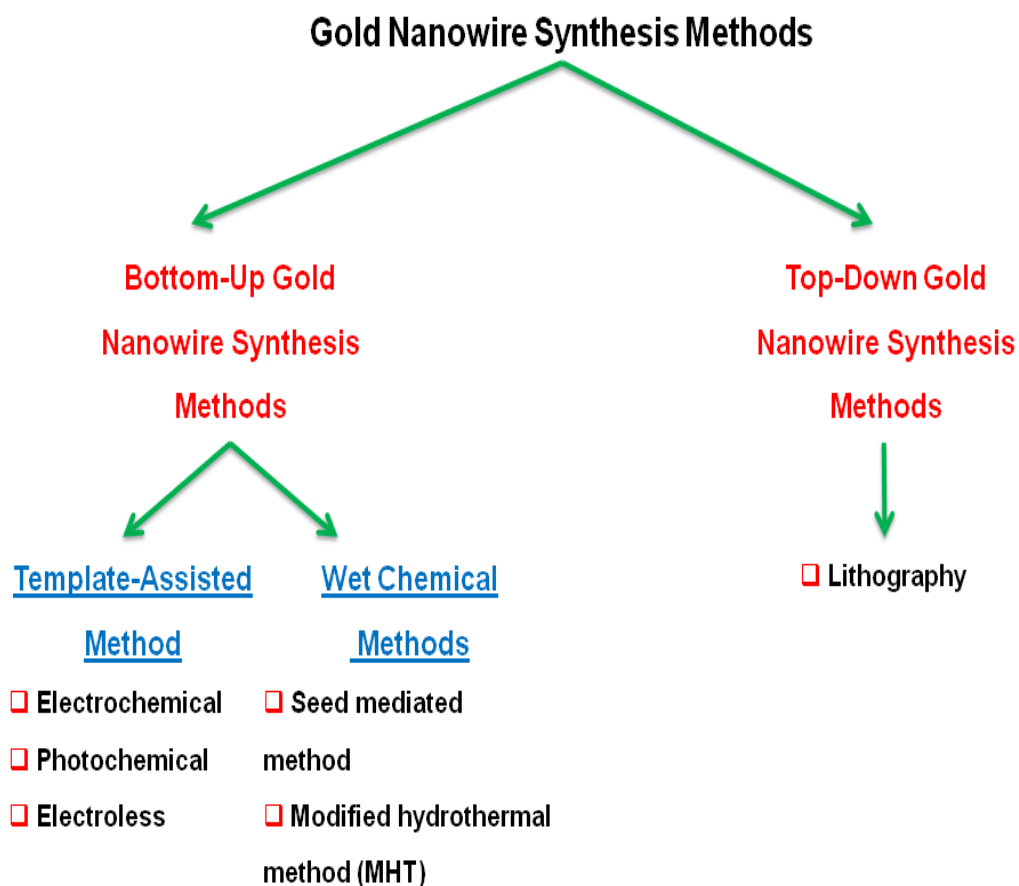


**Figure 6** Au nanowire synthesis methods.

### 2.3.1 Top-Down Gold Nanowire Synthesis Method

#### 2.3.1.1 Lithography

Lithography is the only “top-down” approach in order to form Au nanowires. The most commonly utilized technique for this purpose is electron beam lithography (EBL) (Figure 7). In this procedure, the substrate is coated with an electron-sensitive resist that dissociates into smaller polymer segments when exposed to an electron beam. Then, the resist can be selectively removed with a developing agent. The formation of nanometer-scale openings in the resist through which Au can be deposited is possible with

patterns written with an electron beam. The Au deposited onto the unexposed resist is removed using acetone, which is called lift-off technique. As a result, the formation of intricately shaped nanostructures with dimensional control on the tens of nanometer length-scale is possible. Although lithography is beneficial for nanostructures with unique control over the size, shape and alignment, it does not allow for the synthesis of such structures on macroscopic-length scales. As examples for the other drawbacks; the nanostructures are typically polycrystalline, dimensions less than 10nm are readily obtainable, and nanostructure adhesion to the substrate usually requires an intermediate layer of chromium and titanium [24].

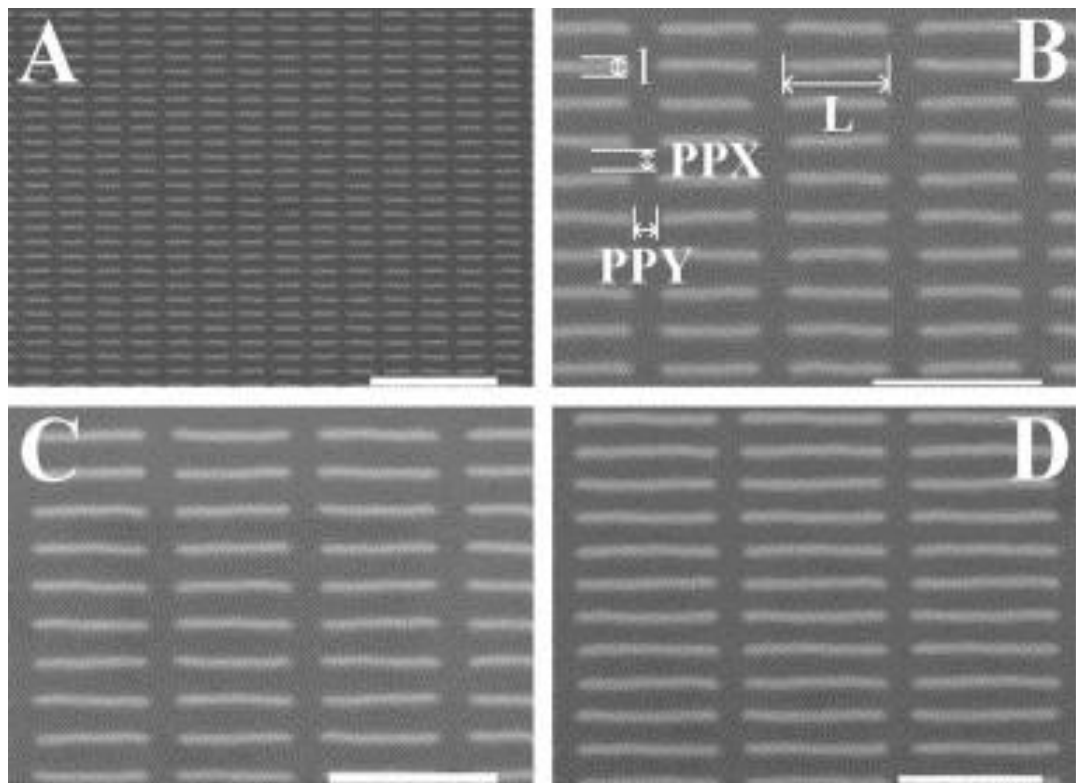


**Figure 7** SEM images of the SERS-active substrates: array of Au nanowires with variable length,  $L$  (A:  $L = 420$  nm, B:  $L = 620$  nm, C:  $L = 720$  nm, D:  $L = 1$   $\mu$ m), 50 nm height, 60 nm width ( $l$ ). The inter-particle spacings are constant

for all arrays and are fixed to 150 nm (PPX and PPY). Scale bars : 2  $\mu\text{m}$  for A and 1  $\mu\text{m}$  for B, C and D [25].

## **2.3.2 Bottom-Up Gold Nanowire Synthesis Method**

### **2.3.2.1 Template Method**

The most widely used Au nanowire fabrication method is the template assisted one which was discovered by Martin and co-workers in early 1990's [26]. Template simply serves as a scaffold within which a different material is generated in situ and shaped into a nanostructure with its morphology complementary to that of the template. [27, 28]

Template method requires either "hard" templates or "soft" templates (Figure 8). Porous anodic alumina films, mesoporous thin films (MTFs), etched ion-track membranes (EITM), mesoporous silica, and porous glass are examples for hard templates. The porous anodic aluminum oxide (AAO) membranes are the most preferable material due to its self-assembled honeycomb array of uniformly sized parallel channels structure [29, 30]. Monolayers, micro emulsions, liquid crystals, vesicles, micelles are utilized as soft templates. Recently, biotemplates (i.e. DNA) have also been used as a soft template for the formation of Au nanowires. Using DNA templates has become very popular in order to prepare Au nanowires due to their specific molecular recognition property and high aspect ratio [5, 31-34]. However, hard templates are more frequently used than ones due to their specific topological stability, veracity, predictability and controllability [35].

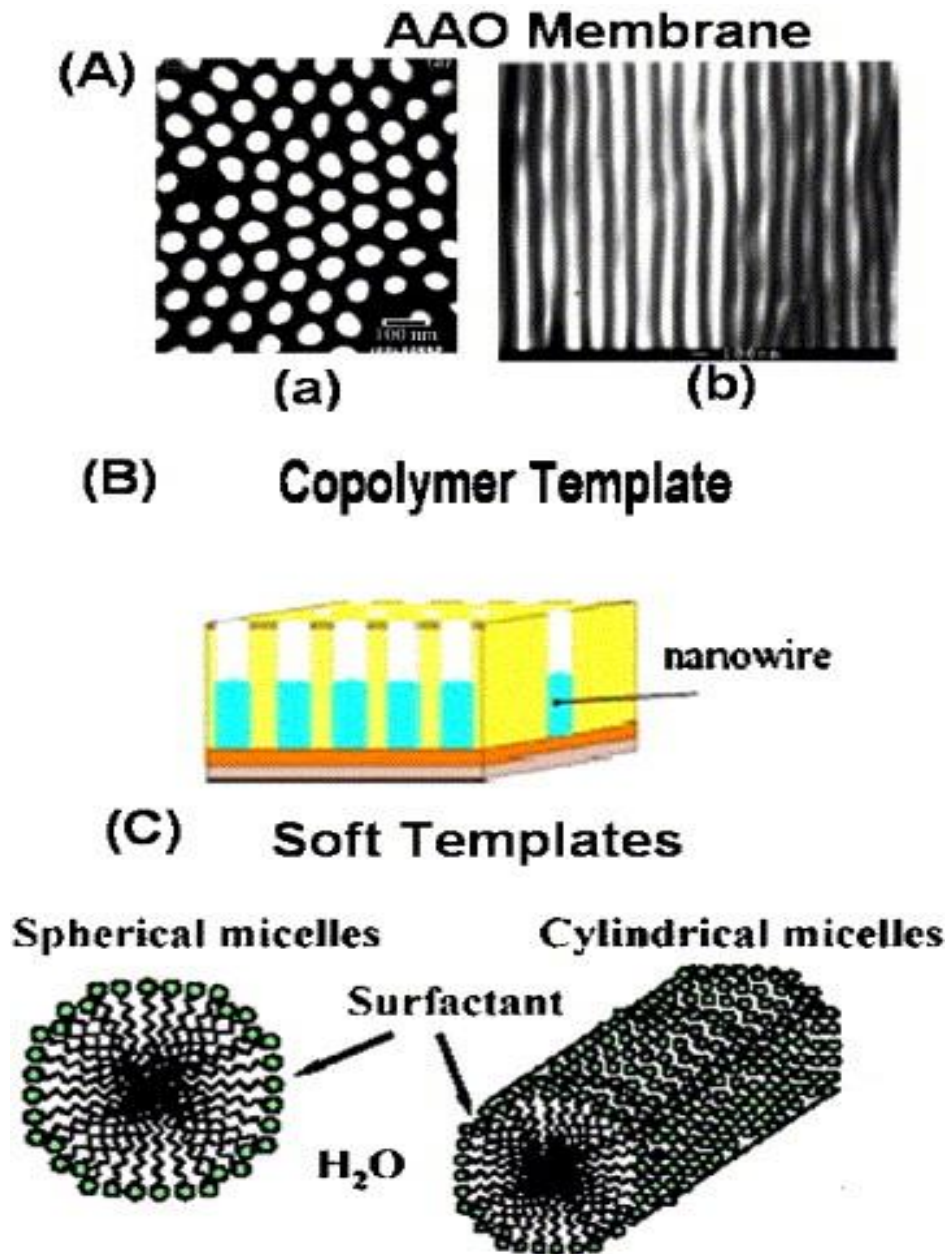


**Figure 8** Schematic illustration of the different templates used in Au nanowire synthesis through template-assisted method; (a) Anodic aluminum oxide (AAO) membrane, (b) Copolymer template and (c) Micelle soft templates [34, 36].

There are some important criteria to choose suitable templates. Chemical stability and mechanical properties of templates are the most important features of templates to be used. The very first and the most critical step in

template assisted method is pore creation. Uniform and parallel pores can be created by the anodic oxidation in the presence of many acids such as sulfuric ( $\text{H}_2\text{SO}_4$ ), oxalic ( $\text{C}_2\text{H}_2\text{O}_4$ ) or phosphoric ( $\text{H}_3\text{PO}_4$ ) acids [37]. Besides, uniformity, density of pores is also very crucial since diameter and length of nanowires strictly depend on them. Therefore, control of nanowire properties can be achieved by manipulation of uniformity and density of pores. Figure 9 demonstrates SEM picture of Au nanowires with 160 nm diameter prepared by template-assisted methods.

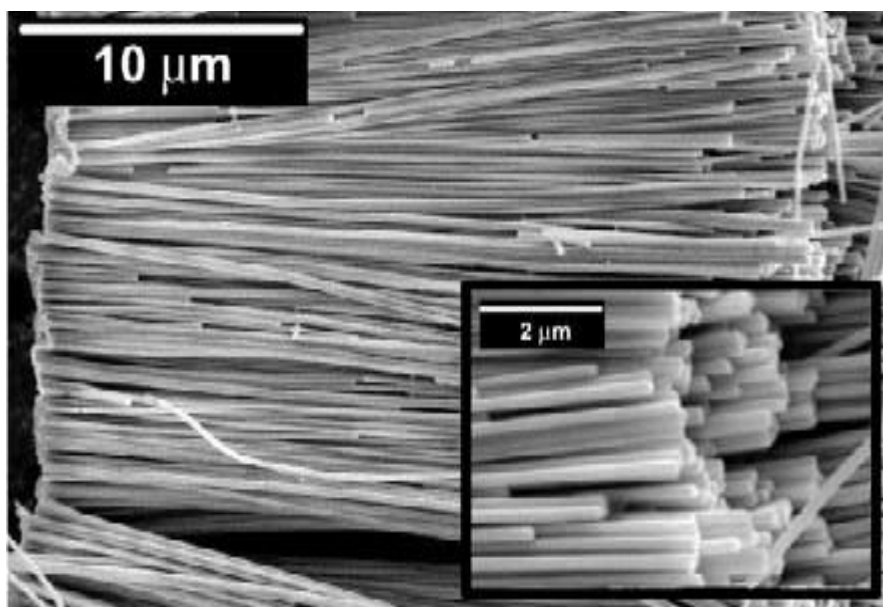


**Figure 9** SEM picture of synthesized Au wires through template-assisted method [29].

After pore creation on template, fabrication of Au nanowires through the method can be achieved by following different routes. These routes are electrochemical, photochemical and electroless methods which differ in way of depositing Au inside the pores of templates.

### 2.3.1.1.1 Electrochemical

Electrochemical deposition is highly preferred method to deposit Au onto templates due to its simplicity. Figure 10 demonstrates an electrochemical deposition cell with three electrodes. These electrodes are Au coated membrane as working electrode, a platinum mesh counter electrode and an Ag/AgCl reference electrode. In this procedure, Au is electrodeposited into the pores of templates using an electrolyte [38]. Crystallinity and crystallographic orientation of Au nanowires can be controlled with important parameters such as temperature, applied voltage, current densities of process [39].

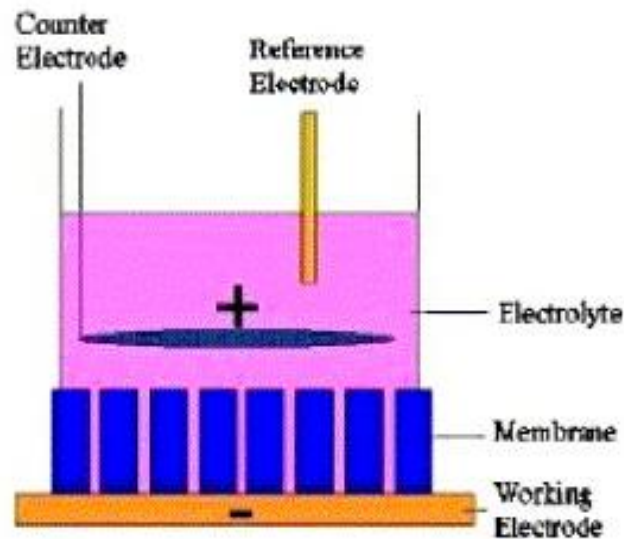


**Figure 10** Schematic illustration of synthesis of Au nanowire through template assisted method modified with electrodeposition [34].

In addition to template assisted method, step edge decoration (ESED) can be modified with electrochemical deposition procedure for fabrication of Au nanowires (Figure 11). Previously, synthesis of metal nanowires including Au with this method could not be achieved. However, with the help of highly oriented pyrolytic graphite (HOPG) crystals, which have very low surface

energy, synthesis of wires can be achieved. Applied convenient nucleation pulse and preoxidized HOPG resulted in an increase of nucleation density along the steps and synthesis of Au nanowires by electrochemical deposition [40].

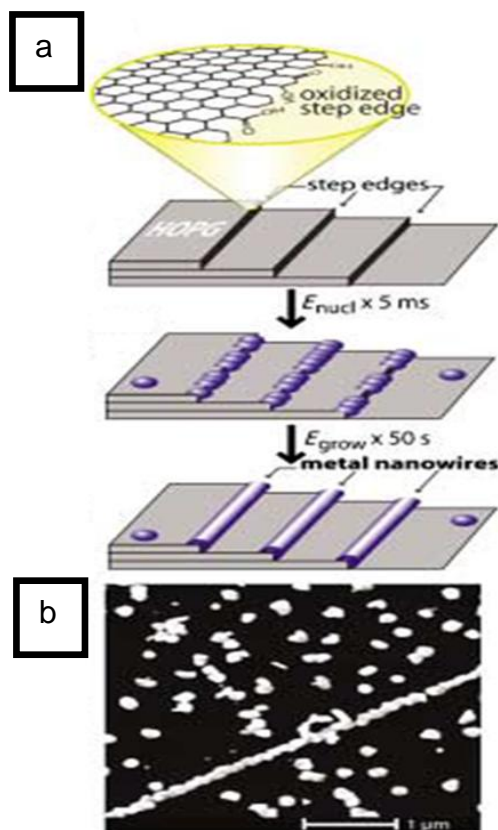


**Figure 11** a)Scheme of synthesis of Au nanowires via step edge decoration, b)SEM image of Au nanowires [40].

#### 2.3.1.1.2 Photochemical

Reducing the metal ions and formation of metal nanostructures under the effect of light is named as photochemical method. This procedure is first reported by Esumi and co-workers in 1995. Modification of the method was done by using different hard and soft templates (Figure 12). Recently, 1D Au nanoparticles have been synthesized by UV-irradiation in rodlike micellar

solution of a cationic surfactant used as a soft template. However, in this method aspect ratio and yield of such materials is very low [41, 42].

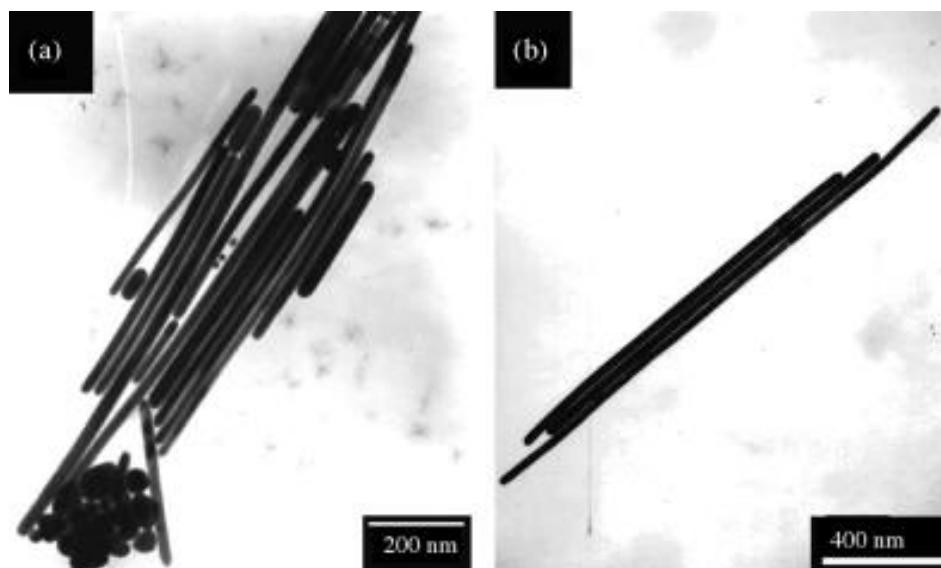


**Figure 12** TEM images of Au nanowires synthesized via template assisted method [41].

### 2.3.1.1.3 Electroless methods

In addition to electrochemical and photochemical methods, electroless method can be employed for the deposition of Au [28]. Being actually a chemical deposition process, electroless deposition involves the use of a chemical agent to coat a material onto the template surface [43]. The electroless deposition does not require the deposited materials to be electrically conductive and deposition starts from the pore wall and proceeds inwardly, whereas deposition begins at the bottom electrode and deposited materials must be electrically conductive in electrochemical deposition. Therefore, hollow fibrils or nanotubes are obtained in electroless deposition, whereas electrochemical deposition results in solid nanorods or nanowires of conductive materials. In electrochemical deposition, the deposition time can

control the length of nanowires and nanorods. However, in electroless deposition the length of the nanotubules is solely dependent on the length of the deposition channels or pores. Different deposition time would mean different wall thickness of nanotubules and an increase in deposition time leads to a thick wall, but sometimes even after a prolonged deposition, the hollow tubule morphology maintains. (Figure 13) [44]. In addition to Au nanotubes, Shi and co-workers achieved to synthesize Au nanowires with high density and high aspect ratio into the channels of mesoporous silica thin films by electroless deposition (Figure 14) [28].

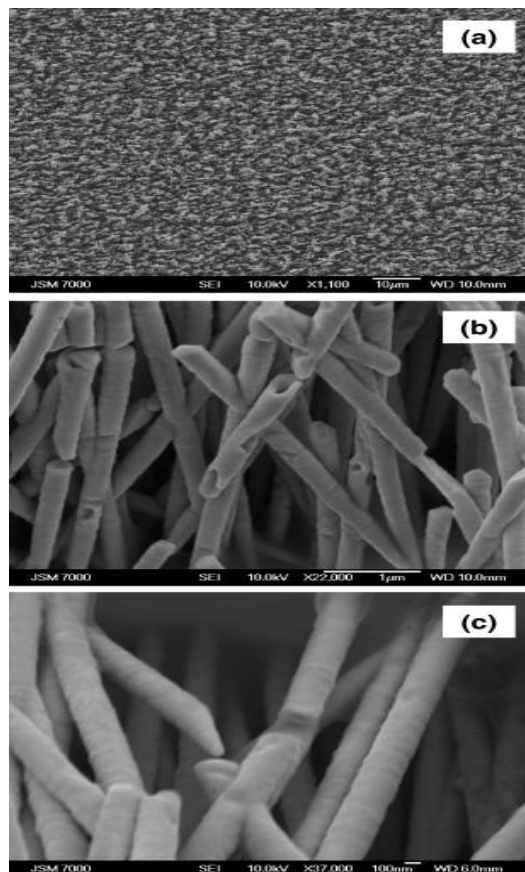


**Figure 13** SEM micrographs of (a) Au nanorod arrays grown in PC membranes covering a large area with uniform size and density, (b) Au nanotubes, ascribed to possible growth propagating along the surface of pore channels, and (c) Au nanorods, attributing to uniform growth from the bottom of pore channels attached to the electrode [44].

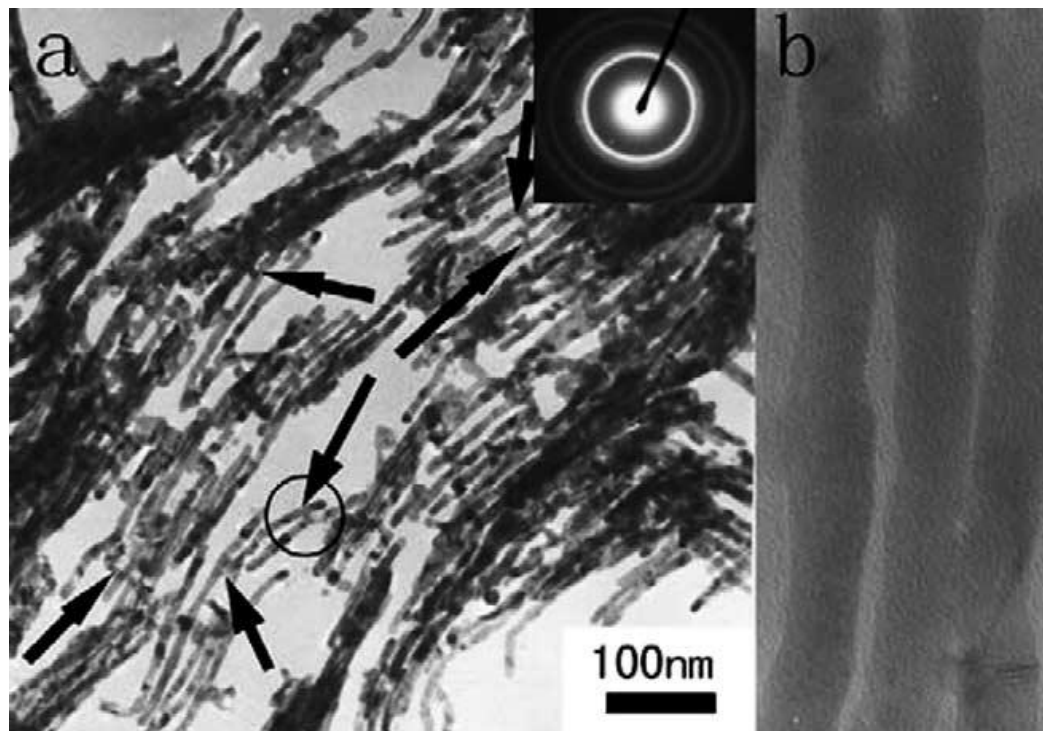


**Figure 14** (a) TEM image of unsupported Au nanowires. (a) The arrows highlight the bridges between the nanowires. The inset shows select-area electron diffraction. (b) The enlarged image of ellipse portion of image [28].

Template assisted method has proven to be an easy process to synthesize Au nanowires with many benefits. For example, it is very simple to control properties of nano structured materials by adjusting the characteristics of template (density, pore diameter). Moreover, low cost and high yield of synthesis make template-assisted method more attractive option for industrial applications [45]. However, separation of Au nanowires from template is generally an important problem and nanowires can be damaged during separation step [46].

### **2.3.1.2 Wet Chemical Methods**

#### **2.3.1.2.1 Seed-mediated Method**

Seed mediated method was first proposed by Wiesner and Wokaun. They obtained anisomeric Au colloids by adding Au nuclei to  $\text{HAuCl}_4$  growth solution in 1989 [47]. Later, many of other researches utilizing this technique have been reported and helped the evaluation of seed-mediated method [48-52]. Jana and C. Murphy are very famous researchers who contribute to the modification of seed mediated method. They achieved to obtain Au nanorods through this procedure in 2001 [53]. Due to the simplicity of the technique, a great control over the quality of resultant structure and flexibility of the process for modifications, the seed mediated growth method has been one of the most widely used way of preparing Au nanomaterials with anisotropic structures.

Seed-mediated process is basically divided into two stages: nucleation and growth of seeds into nanocrystals. In conventional one-step seed mediated method; firstly the crystal seeds are prepared and then the synthesized seeds are added into the growth solution (Figure 15) [54, 55]. Although the method is extensively used for the synthesis of various noble metal nanoparticles, Au nanowires with high aspect ratio and high purity could not be obtained with it. Jana et al. improved the method and named it three-step seed mediated method [56]. In this improved procedure, firstly 3.5-4 nm spherical Au nanoparticles are formed by reduction of Au salt with strong reducing agent (sodium borohydride). Then these Au nanoparticles are used as seeds for second growth, which are sequentially used as seeds for third growth. Later, Kim et al. modified the process which is based on the typical three-step seed-mediated method by reducing the seed concentration. Au nanowires with aspect ratio of ~ 200 were obtained in acidic media where nanowire growth is promoted (Figure 15 (b)) [57]. In both methods, the yield,

monodispersity, size and morphology of Au nanocrystals are affected by many parameters such as seed concentration, reducing agent concentration, temperature, pH, the Au precursor concentration, the surfactant type and concentration, solvent, and even the aging time. The drawback of this method is synthesis of large amount of by-products with not desired morphologies requiring time-consuming purification steps.

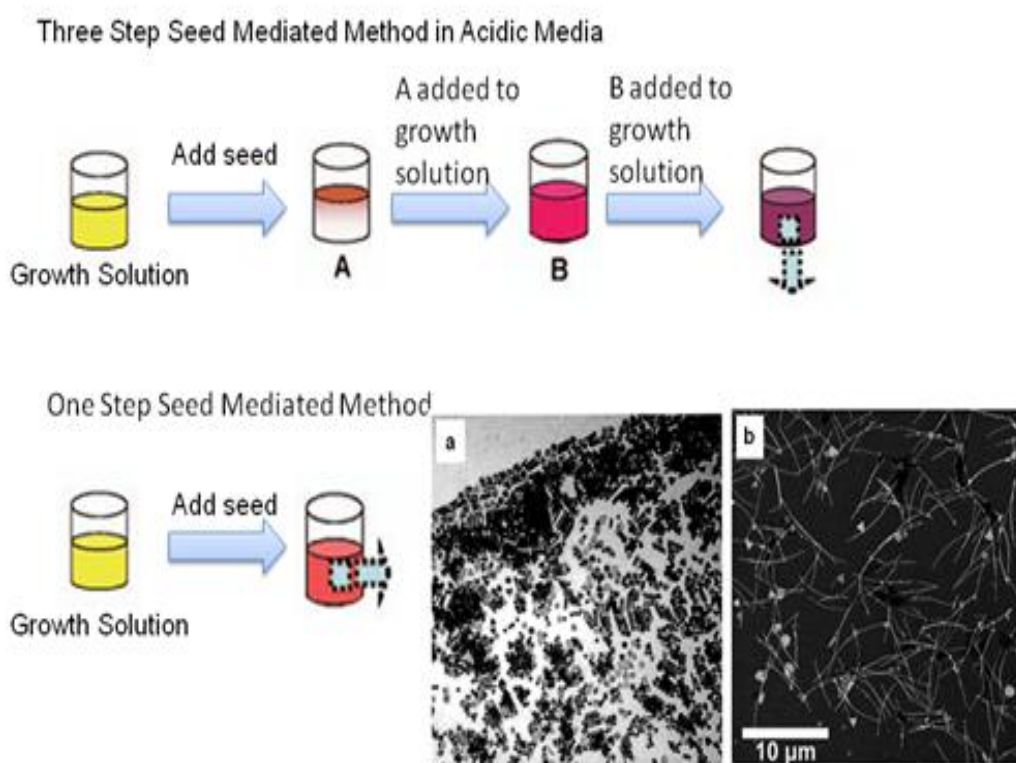


**Figure 15** Schematic illustration of synthesis of Au rod/nanowire through seed mediated method (a) SEM picture of Au nanorods (b) SEM picture of Au nanowires synthesized in acidic media [56, 57].

### 2.3.1.2.2 Modified Hydrothermal Method (MHT)

The term "hydrothermal" usually refers to dissolve and recrystallize (recover) materials from aqueous solvent under high pressure and temperature conditions [58]. To date, pressure and temperature limits are not defined certainly by scientists. However, many researchers endorse an opinion that hydrothermal systems are usually maintained at a temperature above room temperature and pressure greater than 1 atm [58].

Hydrothermal process requires closed system in order to provide appropriate pressure inside the reaction vessel which is capable of resisting to high pressure and temperature even for long reaction times. Generally, autoclaves are used as hydrothermal apparatus (Figure 16). However, thick glass reaction vessels can also be used in some experiments which are conducted under relatively lower pressure.



**Figure 16** Picture of Autoclave [59] .

In this procedure there are very important parameters (i.e. concentration, temperature, pressure, reaction time, etc.) to consider. These parameters have a significant impact on producing desired nanocrystals and affect kinetics of growth process, thermodynamic stability (i.e solubility, reactivity) of the product [58] .

Many papers have been published on investigating temperature and pressure effect in hydrothermal processes [60-64]. Temperature and pressure play collective role on supersaturation and nucleation. Since the reaction is being carried out in a closed container, the vapor pressure above the solution reach to equilibrium after a while at certain temperature. However, a rise in temperature, which also affects the vapor pressure, will increase both the nucleation rate and the linear growth rate hence; the crystallinity of the samples normally increases in time [58].

Reaction time also has a strong effect on the morphology control of the resulting products. Recently, it was reported that titanate nanotubes can be transformed into nanoribbons depending on critical treatment duration [65].

Hydrothermal process can be effective in producing many kinds of nanocrystalline materials including ZnO [66], Hap [67], TiO<sub>2</sub> [68], CeO<sub>2</sub> [69], SnS<sub>2</sub> [70], CoFe<sub>2</sub>O<sub>4</sub> [71]. Recently, Pal and co-workers modified the conventional hydrothermal process by using a screw capped test tube instead of using autoclave. Additionally, tungsten light is fitted to a closed wooden box which is utilized as heat source (Figure 17). Through this modified method not only Au nanowires (Figure 18) [23] but also nanoplates of CuS [72], ZnO nanococoons [73], Fe<sub>3</sub>O<sub>4</sub> nanowafers [74], and different nano-structures such as nanoflowers, nanopetals, nanopillars, nanorods, nanobundles of TiO<sub>2</sub> (Figure 19) have been successfully synthesized [75].

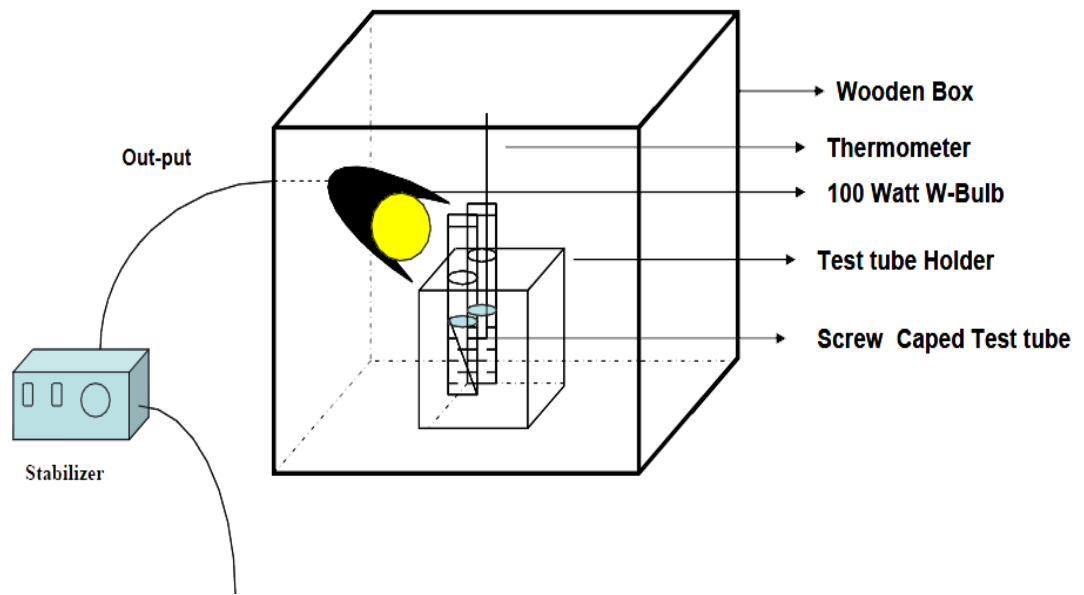


**Figure 17** Tungsten light-bulb fitted setup [75].

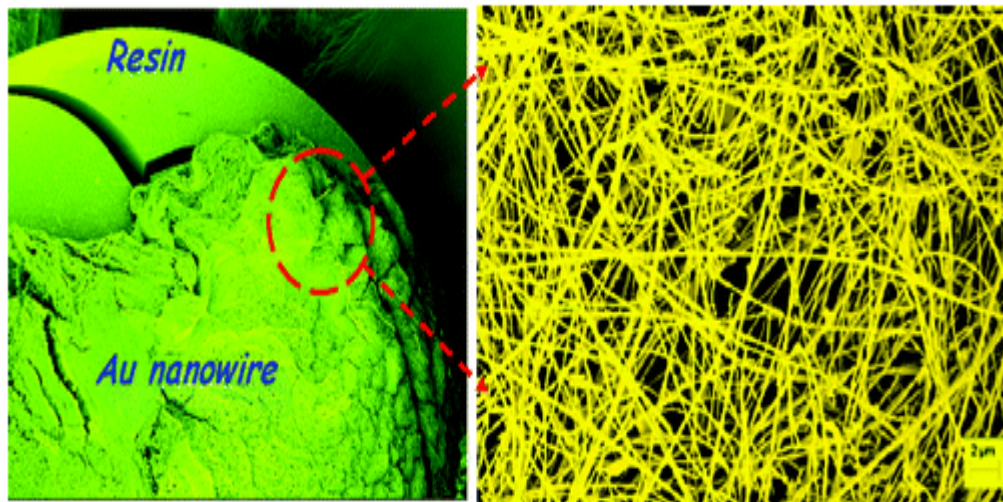


**Figure 18** Micrometer long Au nanowires [23].

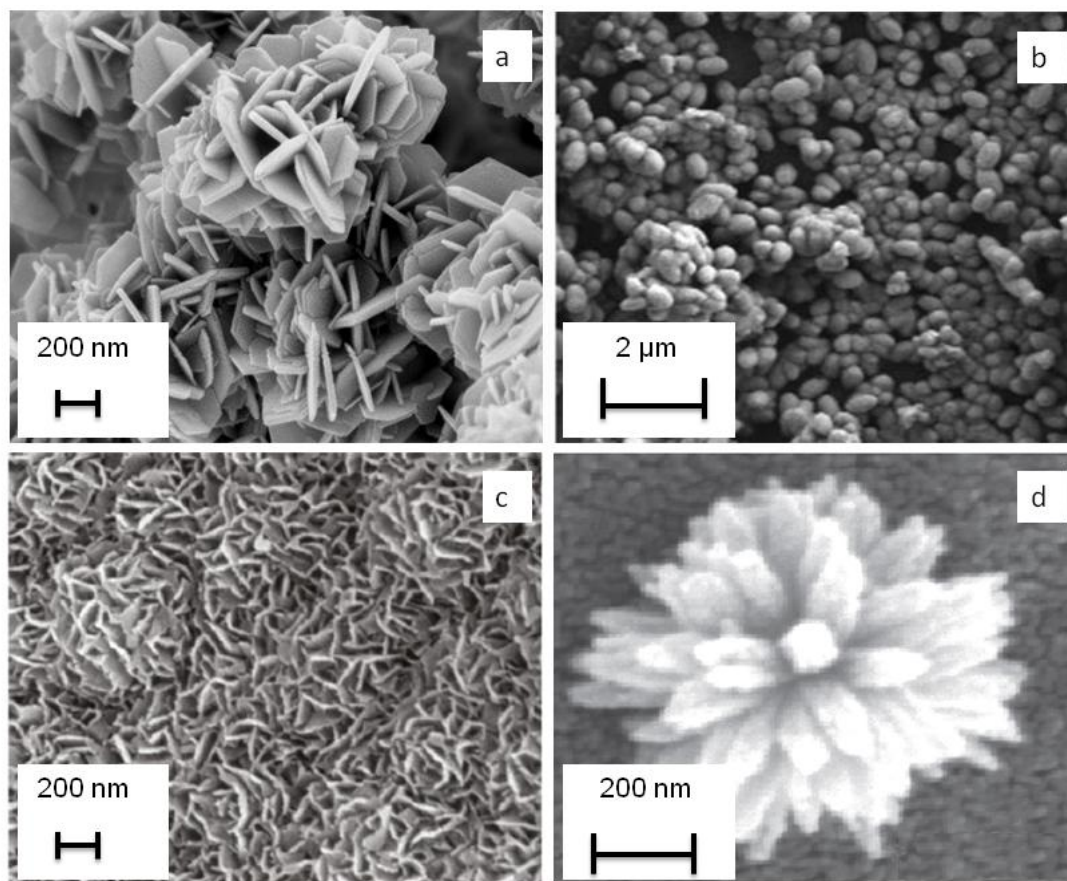


**Figure 19** SEM images of different types of nanostructures via modified hydrothermal method (a) CuS nanoplates (b) ZnO nanococoons (c) Fe<sub>3</sub>O<sub>4</sub> nanowafers (d) TiO<sub>2</sub> nanoflowers [72-75].

In order to synthesize Au nanowires, this new modified process involves two steps: (i) the deposition of Au ions on the anion exchange resin, (ii) the reduction of Au (III) in the presence of surfactant at high temperature. Figure 16 shows large amount of product which consists of micro-meter long Au nanowires synthesized with MHT.

## **2.4 Comparison of Modified Hydrothermal Process with the Conventional Methods**

Top-down methods are very expensive compared to other procedures because it requires an intermediate layer of chromium or titanium in order to prevent the adhesion of nanowires to the substrate. Moreover, it is very difficult to obtain nanostructured materials with control over the size, shape and alignment. Some bottom-up methods require complex equipments. For instance, electrochemical cells, anode-cathode plates in electrochemical method make this route complicated. Additionally, requirement of suitable template and uncontrolled creation of pores are the main disadvantages of template assisted method. Moreover, difficulty in removal of the template from synthesized nanowires is another important problem in template method. Although, seed-mediated method is very popular, the synthesis of high aspect ratio Au wires is very difficult. Recently, researchers improve a new approach that is called three-step seed mediated method. However, polydispersity of product increases and time consuming purification steps are required in this method. On the other hand, modified hydrothermal process stands out in all of these important concerns. It is a rather new Au nanowire fabrication method that provides simple process setup, cost effective and solution based alternative that enables synthesis of micro-meter long, very pure Au nanowires in gram quantity. Considering these crucial benefits, modified hydrothermal process is expected to become the leading process to synthesize very long, pure Au nanowires.

## CHAPTER 3

### EXPERIMENTAL

#### 3.1 Materials

All chemicals; gold (III) chloride trihydrate ( $\text{HAuCl}_4 \cdot 3\text{H}_2\text{O}$ ), ethylenediaminetetraacetic acid ( $\text{Na}_2\text{-EDTA}$ ), hexamethylenetetramine (HTMA), Amberlite IRA-400 (Cl) ion-exchange resin were purchased from Sigma-Aldrich and used without further purification. Deionized (DI) water (18 M $\Omega$ ) was used throughout all experiments.

#### 3.2 Methods

A solution of 1mM  $\text{HAuCl}_4$  was prepared by dissolving 0.039 g of gold (III) chloride trihydrate ( $\text{HAuCl}_4 \cdot 3\text{H}_2\text{O}$ ) in 10 mL DI water. Gold (III) ions were immobilized on anion exchange resin by adding 0.125 g Amberlite IRA-400 (Anion Exchange Resin) to the Au solution and mixing for 30 minutes (Figure 20 (a)). The color of the solution turned from yellow to colorless, and colorless beads became yellowish indicating the anion exchange process was completed successfully. (Figure 20 (b)) Next, resin beads were washed seven times with 5 mL DI water to remove the excess  $\text{AuCl}_4^-$  that are not immobilized on surface of the resin. Synthesis of desired Au nanowires was achieved at optimum conditions derived after the parametric study. Briefly, 0.03 M  $\text{Na}_2\text{-EDTA}$  (0.3 M for HMTA) was added to the test tube and heated

for 4 hours in oil bath at 125 °C (110 °C for HMTA). Formation of thick brown colored layer indicates the synthesis of Au nanowires. (Figure 20 (c), (d)) The parameters used in the experiment: i) concentration of surfactant molecules: 0.03 M, 0.05 M, 0.1 M, 0.3 M, 0.5 M of HMTA and 0.01 M, 0.03 M, 0.1 M, 0.3 M of Na<sub>2</sub>-EDTA, ii) reaction temperature: 70 °C, 90 °C, 110 °C, 125 °C, and iii) reaction time: 10 min, 30 min, 2 h, 4 h, and 5 h for both surfactant molecules (HMTA, Na<sub>2</sub>-EDTA). Throughout the parametric study, only one parameter was changed, while the others were kept constant.

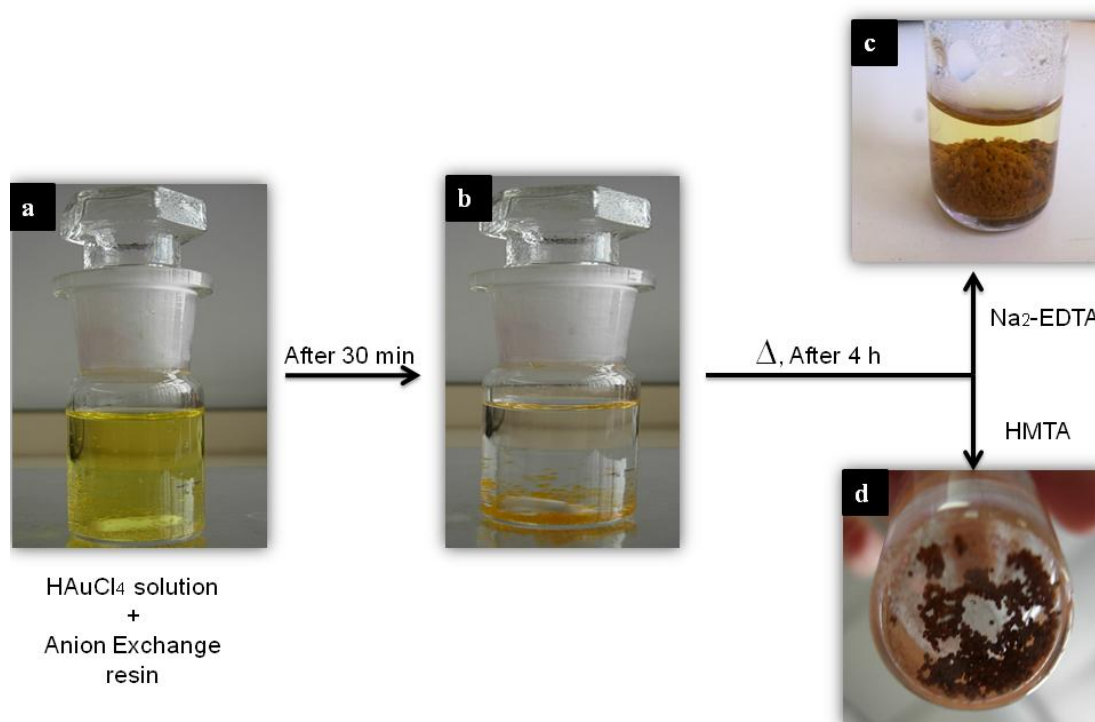


**Figure 20** Photographs of (a) mixture of HAuCl<sub>4</sub> solution (yellow colored) with anion exchange resin (colorless beads) (b) Au ions are deposited onto anion exchange resin (color became orange) after 30 minutes of stirring; as-synthesized Au nanowires in the presence of (c) Na<sub>2</sub>-EDTA and (d) HMTA after 4 hours of heating.

### **3.3 Characterization**

Scanning electron microscopy (SEM) studies were acquired using FEI Nova Nano SEM 430 microscope operated at 10 kV. High-resolution transmission electron microscopy (HRTEM) was performed on a JEOL TEM 2100F microscope operating at 200 kV. X-ray diffraction (XRD) measurements were done on a Rigaku D/Max-2000 pc diffractometer with Cu K $\alpha$  radiation ( $\lambda = 1.54 \text{ \AA}$ ) operating at 40 kV. PHI-5000 Versaprobe, equipped with aluminum K $\alpha$  at 1486.92 eV X-ray source was used to perform X-ray photoelectron spectroscopy (XPS) analyses.

## CHAPTER 4

### RESULTS AND DISCUSSION

#### 4.1. Introduction

In this thesis, Au nanowires with very high aspect ratio were prepared through modified hydrothermal procedure (MHT). This method is adapted from the work of Sinha et al. [23], however, we have modified their method by changing the way of heating the reaction vessel. In order to obtain uniform heat distribution, we have conducted our experiments by placing reaction vessel in an oil bath heated by a hot plate instead of using light bulb. Using oil bath enables a good control over reaction temperature and significant increase in product yield. Moreover, we observed that using different surfactant molecule such as HMTA also results in formation of Au nanowires. The use of HMTA as a structure directing agent was previously reported extensively for the synthesis of ZnO nanowires through hydrothermal route [66, 76-79]. There are also a few reports on the use of the molecule in Au nanoparticle synthesis [80, 81]. However, this is the first use of the surfactant molecule for the synthesis of Au nanowires. Na<sub>2</sub>-EDTA and HMTA have amine group that is responsible for reduction of Au (III) ions and growth of Au nanowires under modified hydrothermal process. Also, we have investigated effect of surfactant concentration, temperature and reaction time for both surfactant molecules, HMTA and Na<sub>2</sub>-EDTA. It was observed that these parameters play crucial roles on the morphology, yield and structural purity of the materials synthesized.

## 4.2. Deposition of Au Ions onto Resin and Their Reduction Process

An anion exchange resin was used to immobilize  $\text{AuCl}_4^-$ . Anion exchange resins involve a polymer backbone with quaternary ammonium groups as an integral part of the polymer lattice with electric charges that are neutralized by the charges carried by the counter ions [23]. In this study, Amberlite IRA-400 (chloride form) anion exchange resin was used. The resin provides the deposition of Au ions which have positive charge on it by exchanging the anion ( $\text{AuCl}_4^-$ ) with the ones ( $\text{Cl}^-$  anions) on the resin matrix. After immobilization of  $\text{AuCl}_4^-$  anions, formation of Au nanowires was achieved by reduction of Au (III) ions by surfactant molecules which are also acting as structure directing agent [23].

Throughout the reduction and growth process of Au nanowires, at first, sphere like Au nanoparticles are formed on resin matrix (Figure 21 (a)). Later, they are polarized by anion exchange resin which has negative charge. These polarized particles start the chain structure and become incentive factor for the formation of Au nanowires. During the reaction occurrence, synthesized Au nanoparticles are attached each other one by one via electrostatic field force. In addition to electrostatic field force, dipole-dipole attraction between Au nanoparticles has also lead to the formation of Au nanowires (Figure 21 (b)).

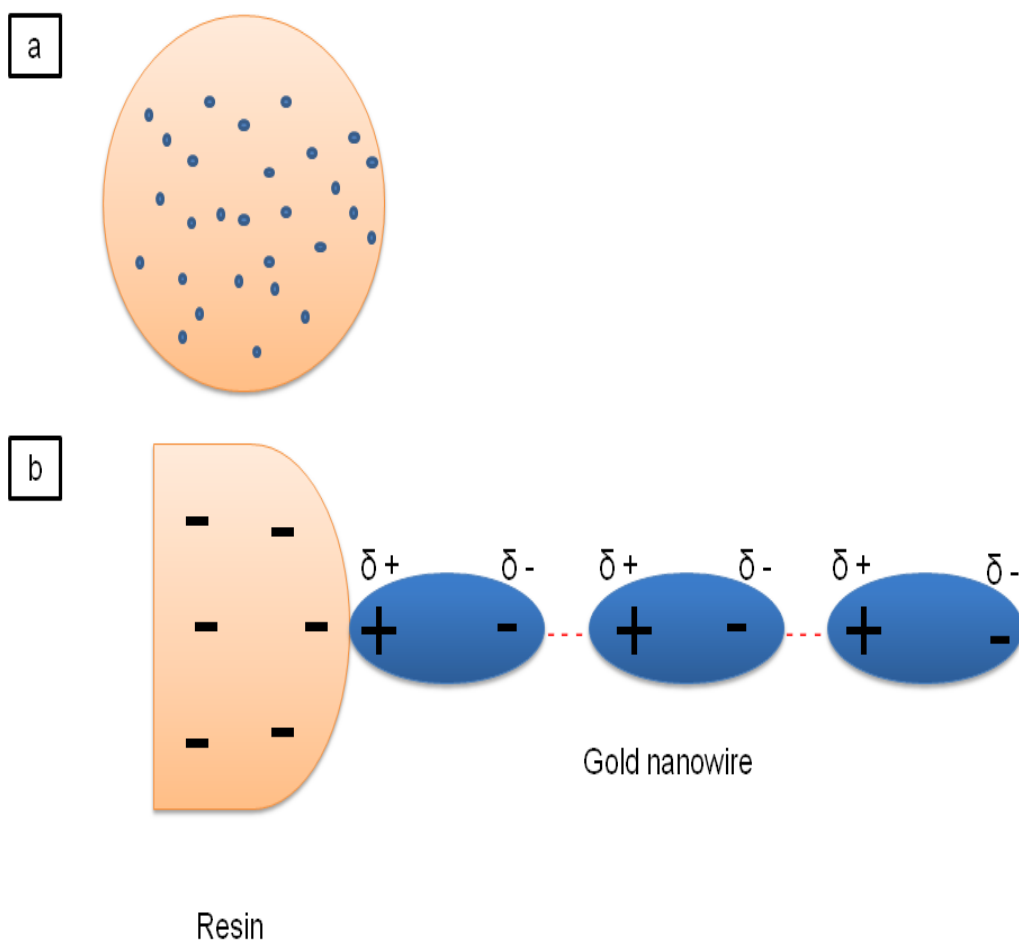


**Figure 21** Schematic illustration of (a) deposition of Au ions onto anion exchange resin (b) growth process of Au nanowires through electrostatic field force and dipole-dipole interaction.

Figure 22 and Figure 23 shows characterization results of Au nanowires prepared in the presence of HMTA and Na<sub>2</sub>-EDTA, respectively. These results are for the nanowires synthesized at optimum reaction conditions that are determined after the parametric study as surfactant concentration of 0.3 M for HMTA, 0.03 M for Na<sub>2</sub>-EDTA, reaction temperatures at 110 °C for HMTA and 125 °C for Na<sub>2</sub>-EDTA, and 4 hours of reaction time for both molecule. Figure 22 (a) and Figure 23 (a) indicate SEM image of Au nanowires with high aspect ratio and 50-100 nm diameters are obtained with HMTA and Na<sub>2</sub>-EDTA, respectively. It should be noted that synthesized Au

nanowires are bundled. During the separation of nanowires from the bead surface, they break as a result of sonication process. Therefore the maximum length of nanowires could not be measured.

XRD analysis confirmed the crystal structure of Au nanowires. Figure 22 (b) and Figure 23 (b) illustrates XRD patterns of Au nanowires prepared with HMTA and Na<sub>2</sub>-EDTA, respectively. For both surfactant molecules, four peaks were appeared at  $2\theta$  of  $38.4^\circ$ ,  $44.6^\circ$ ,  $64.78^\circ$  and  $77.74^\circ$ , which can be assigned to the diffractions of the (111), (200), (220), (311) planes, demonstrating the face-centered cubic (fcc) metal Au structure was formed (JCPDS Card No. 65-2870) [82]. The lattice parameter of Au nanowires was calculated by UNIT CELL software and found as 4.073Å, which is very close to that of bulk Au material (JCPDS Card No. 65-2870) [83]. The relatively high intensity of (111) diffraction peak suggests that Au nanowires has a crystal structure dominated by (111) facets.

The product was further characterized by XPS analysis. As shown in Figure 22 (c) and Figure 23 (c) the XPS spectra demonstrates of two sharp peaks appeared at 82.5 and 86.2 eV for HMTA supported nanowires and 82.9 eV and 86.5 eV for Na<sub>2</sub>-EDTA supported nanowires, corresponding to the Au 4f<sub>7/2</sub> and Au 4f<sub>5/2</sub> components, respectively. The results agree well with the previously reported XPS results for pure metallic Au [84].

TEM images of typical nanowires are shown in Figure 22 (d) and Figure 23 (d) for both surfactant molecules. Insets show high-resolution TEM (HRTEM) image as well as selected area diffraction (SAED) pattern recorded from the nanowires. The observed diffraction rings and interplanar spacing for lattice fringe of 0.247 nm and 0.232 nm for HMTA and Na<sub>2</sub>-EDTA, respectively, corresponds to the (111) lattice plane of face-centered cubic (fcc) Au [85-87].

Strong signals of Au were observed in EDS analyses as shown in Figure 24 for HMTA and Na<sub>2</sub>-EDTA, respectively.

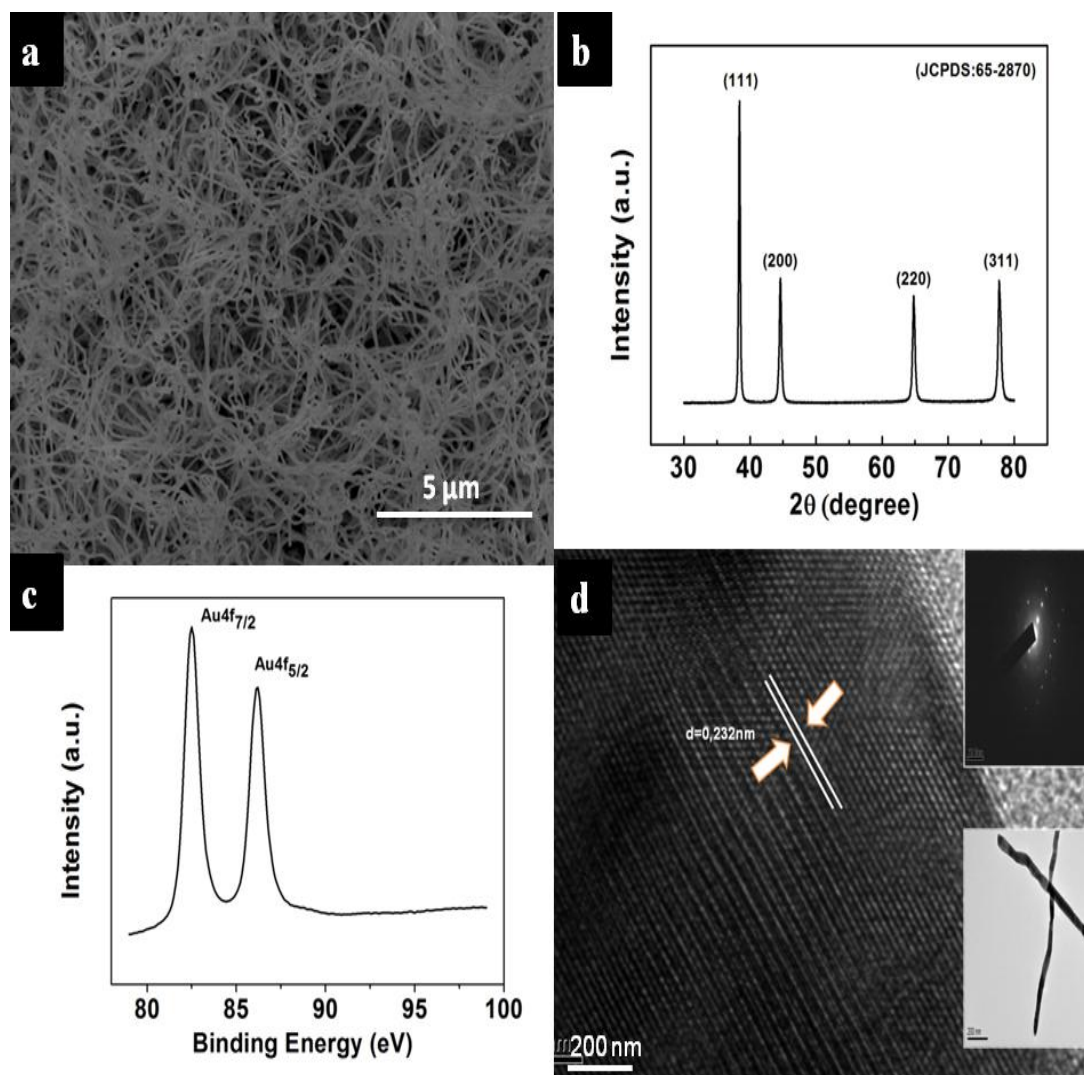


**Figure 22** Characterization of Au nanowires synthesized with HMTA (a) SEM images, (b) XRD pattern, (c) XPS spectra and (d) TEM image. Inset shows HRTEM image and SAED pattern for the nanowires.

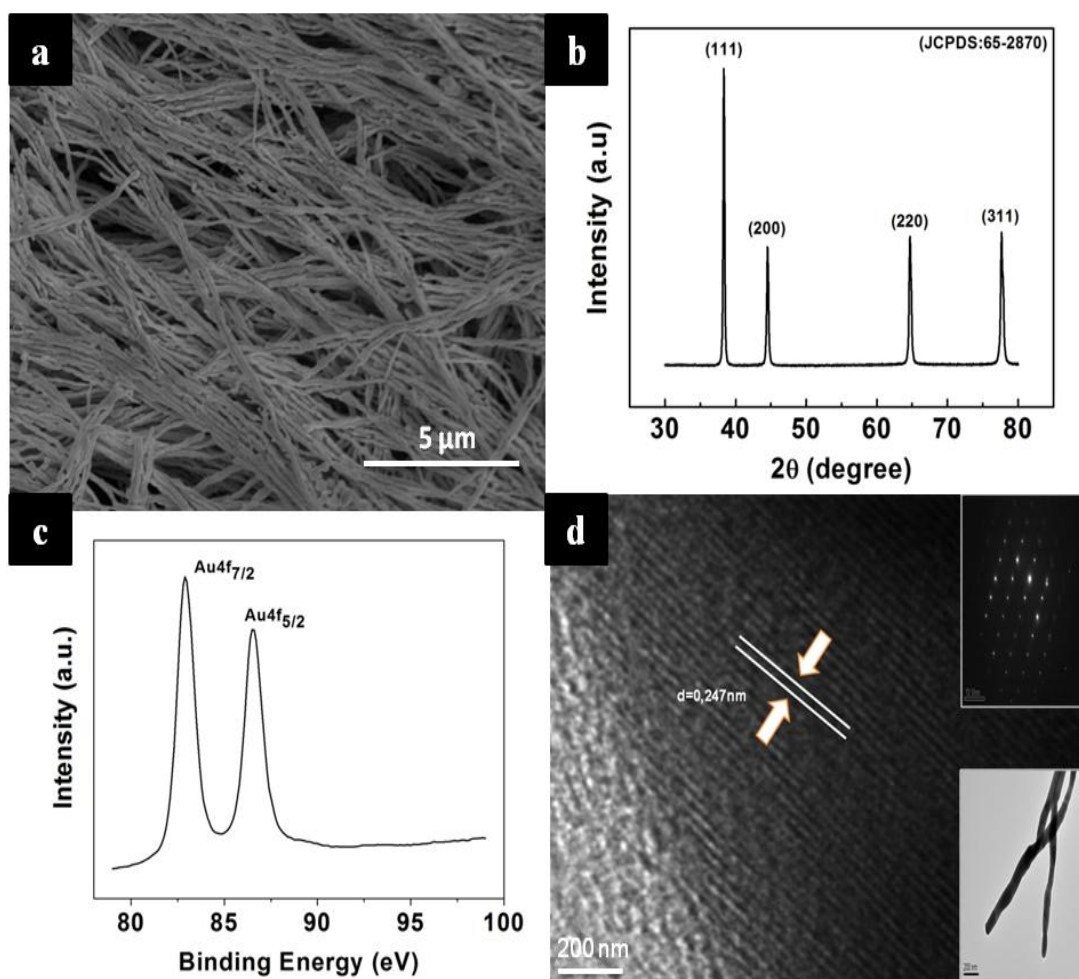


**Figure 23** Characterization of Au nanowires synthesized with Na<sub>2</sub>-EDTA (a) SEM images, (b) XRD pattern, (c) XPS spectra and (d) TEM image. Inset shows HRTEM image and SAED pattern for the nanowires.

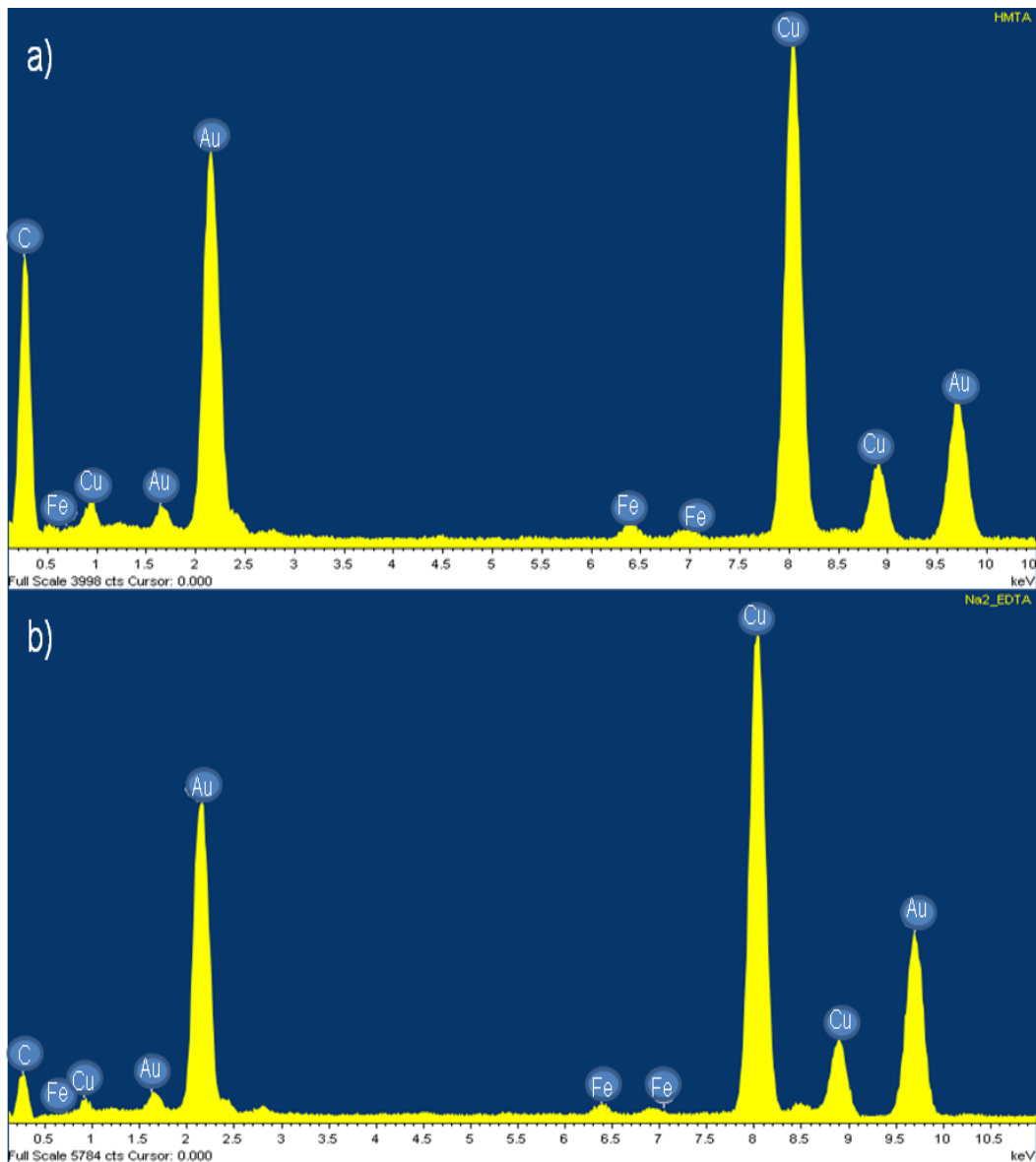


**Figure 24** EDS analysis of synthesized Au nanowires in the presence of (a) HMTA and (b) Na<sub>2</sub>-EDTA.

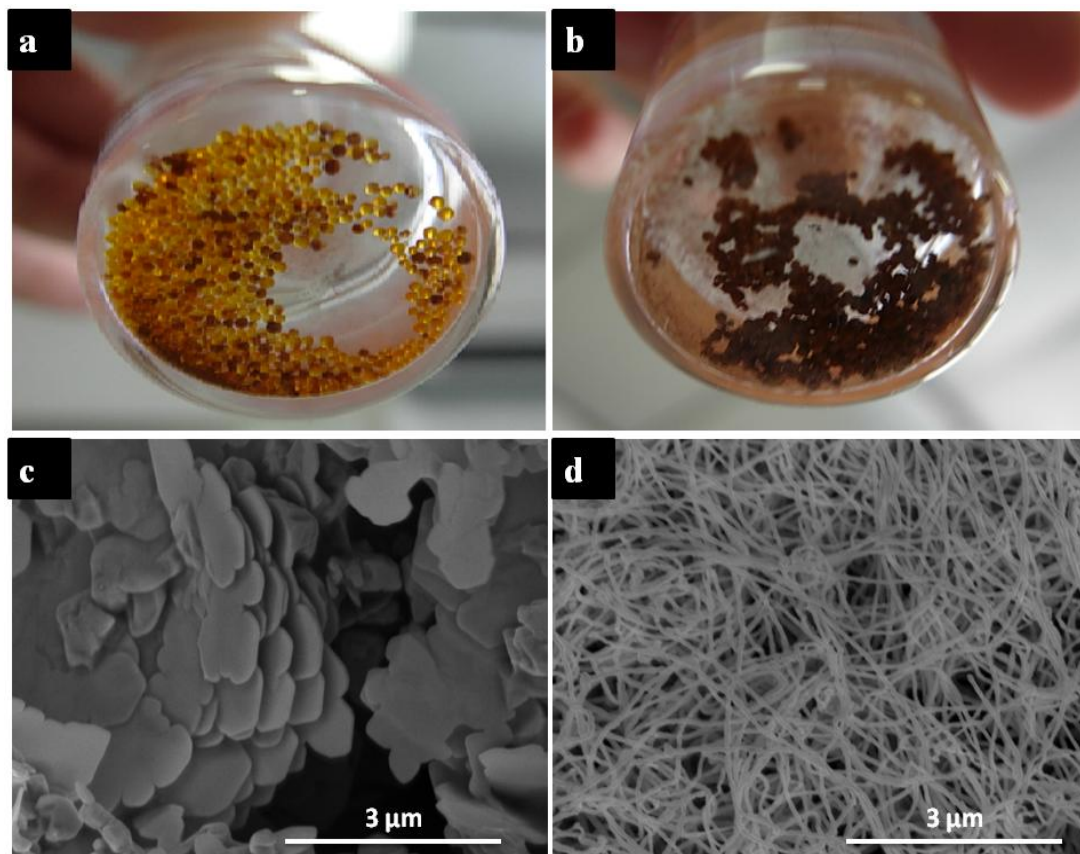
The synthesis of Au nanowires with MHT method requires optimization of reaction parameters such as type and concentration of reagents, temperature and reaction time systematically to maintain high quality nanowires. Throughout the parametric study on Au nanowire growth as one parameter is being investigated others were kept constant. The results of the study on the reaction parameters are presented in following sections.

### **4.3. Determination of the Modified Hydrothermal Process Parameters**

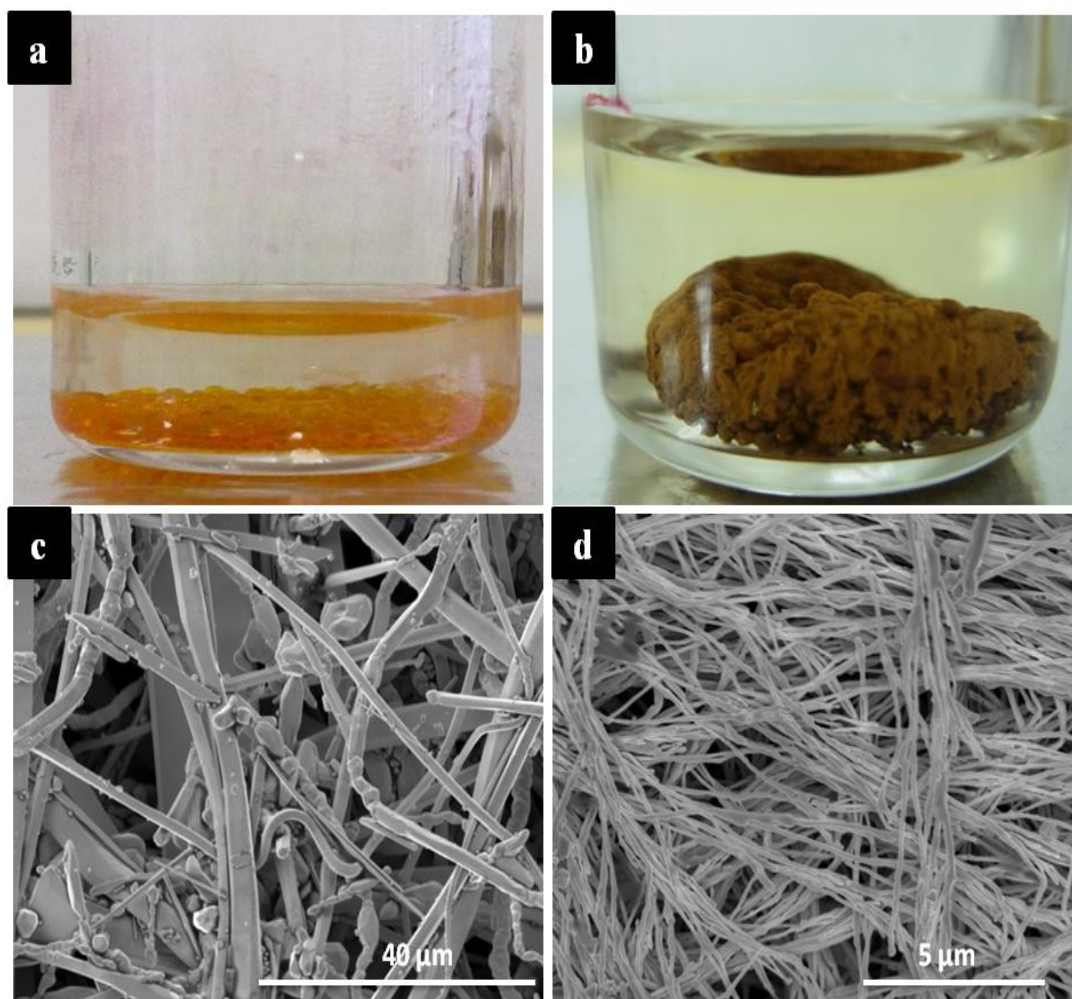
#### **4.3.1 Effect of Surfactant**

Surfactants are essential in nanomaterials synthesis. They provide dynamic, protective shell which stabilize the nanomaterial against aggregation and mediate nucleation and growth processes [55, 88]. Therefore, using the right surfactant in appropriate amount is crucial for controlling the size and the shape of nanomaterials as well as for preparing high quality materials. In modified hydrothermal process, reduction and growth of Au ions is achieved on the resin surface by HMTA and Na<sub>2</sub>-EDTA. As mentioned above, both of these chemicals have ammine groups which serve as reducing agent as well as growth controlling agent. Therefore, concentration of surfactant is critical for the growth of nanowires. High enough concentrations of surfactant are needed for making nanowires in desired quality and morphology.

In the procedure used, the concentration of Au ions is limited by the ion exchange capacity of the resin (3.5 mmol/g for AuCl<sub>4</sub><sup>-</sup> ions) [23]. Additionally, ratio between concentration of Au ions and surfactant is very crucial for the progress of the reaction. When there is insufficient amount of surfactant, reaction does not take place and growth process which is assisted by the surfactant molecule could not be completed and nanowire formation may not be observed (Figure 25 (a)-(d) and Figure 26 (a)-(d)). Since the growth process will continue until the Au supply depletes, optimum concentration of surfactant is needed for making nanowires in desired size, shape, and purity.



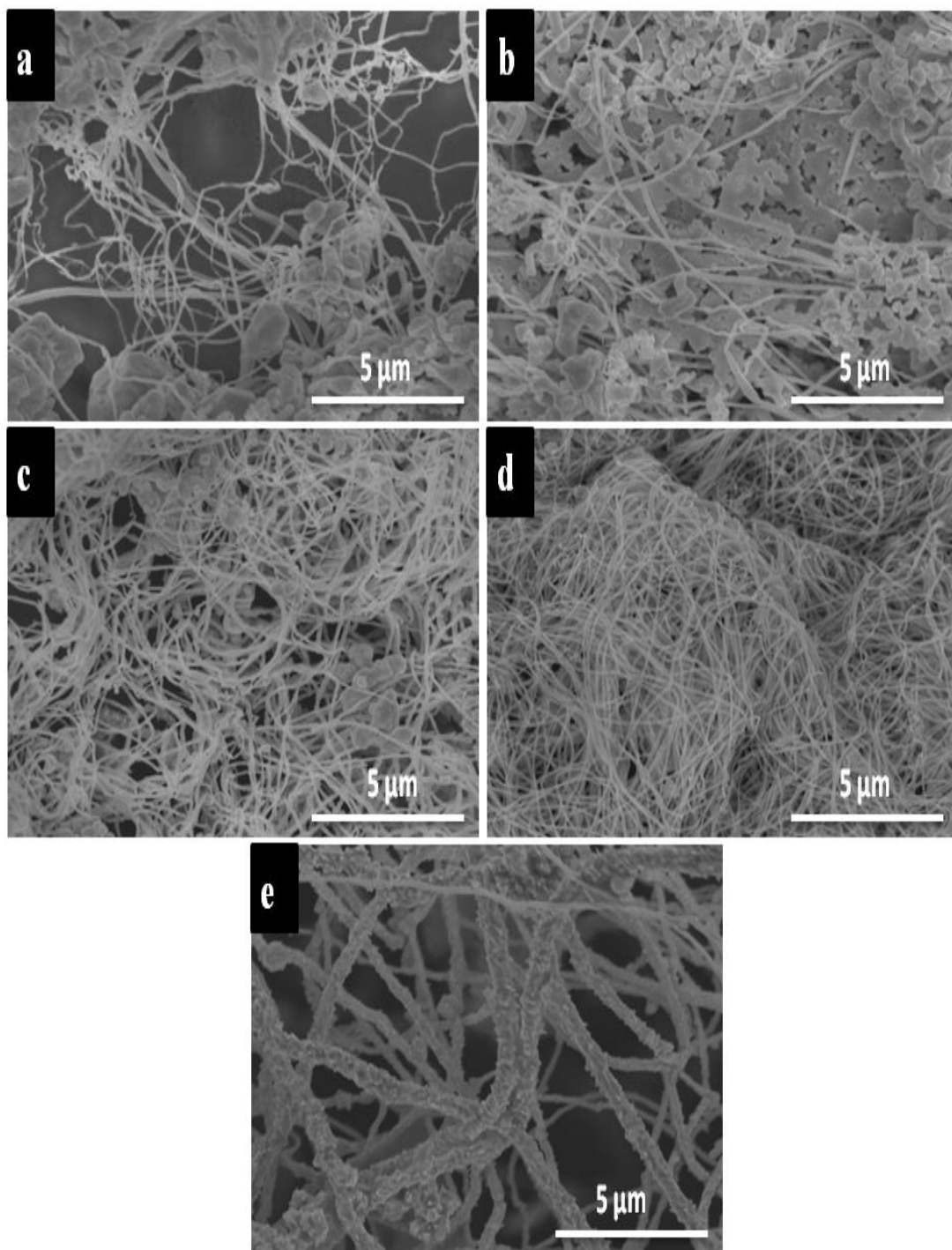
**Figure 25** (a) Au micro structures synthesized with HMTA lower than optimum amount (b) Au nanowires synthesized with sufficient amount of HMTA (c) SEM image of micro structures (d) SEM image of nanowires.



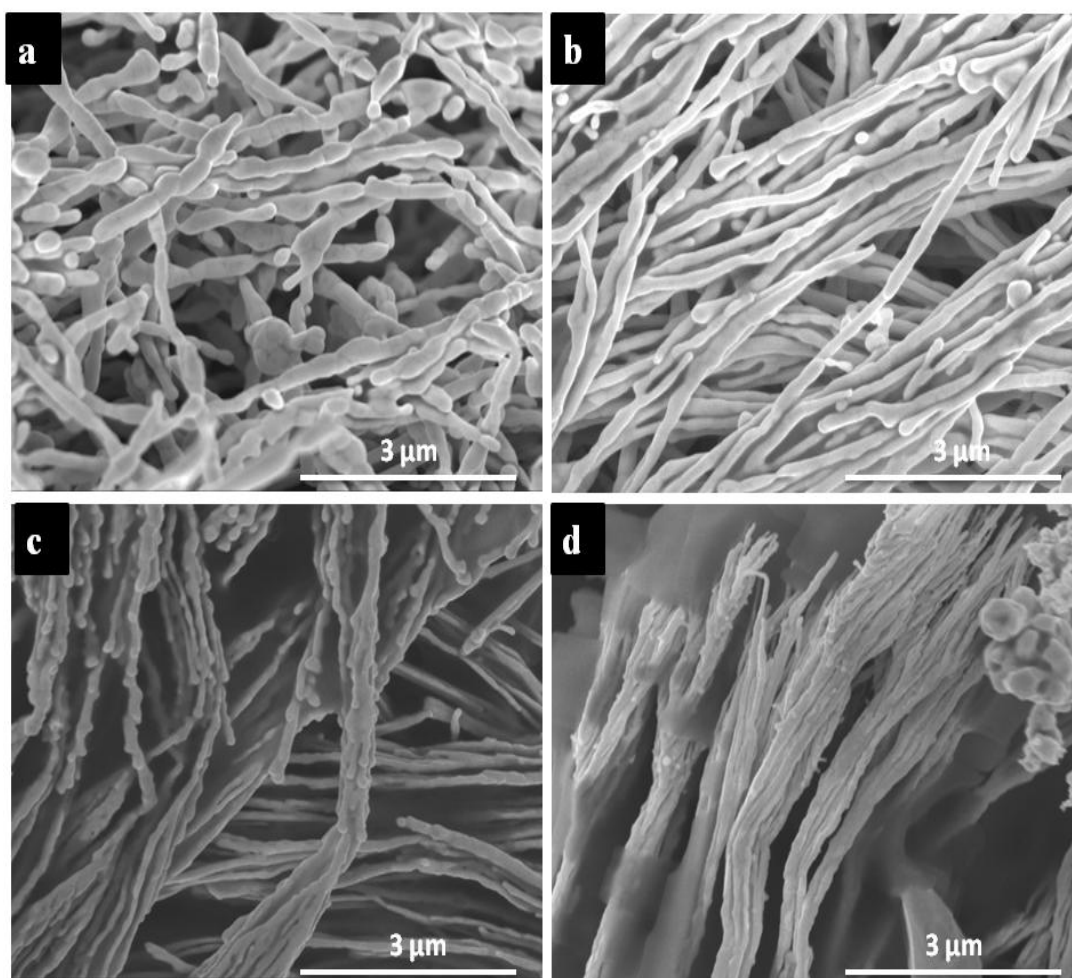
**Figure 26** (a) Au micro structures synthesized with  $\text{Na}_2\text{-EDTA}$  lower than optimum amount (b) Au nanowires synthesized with sufficient amount of  $\text{Na}_2\text{-EDTA}$  (c) SEM image of micro structures (d) SEM image of nanowires.

Figure 27 and Figure 28 demonstrates the Au nanowires synthesized from the use of various concentrations of HMTA (0.03 M, 0.05 M, 0.1 M, 0.3 M, 0.5 M) and  $\text{Na}_2\text{-EDTA}$  (0.01 M, 0.03 M, 0.1 M, 0.3 M). The nanowire synthesis is observed at all concentrations of both surfactant molecules; however, morphology, yield and structural purity vary significantly with surfactant concentration. This change is more notable when HMTA was used (Figure 27 (a) – (e)). Below 0.3 M, beside Au nanowires micron-sized other shapes are formed. Moreover, synthesized wires do not have uniform diameter at this

surfactant concentration. The observation suggests that inadequate amount of surfactant exist in the media to direct nanowire formation. The nanowire synthesis was improved considerably with the increase in surfactant concentration. The highest yield and structural purity was obtained at an HMTA concentration of 0.3 M, which is determined as the optimum concentration for synthesis of desired nanowires. Increase of the concentration to 0.5 M lead to significant increase in diameter of nanowires and change in the morphology of their surface. Smooth surface of nanowires become spiky at this concentration. This is most likely due to continue of the growth process with additional supply of surfactant and dissolution of some of the Au nanoparticles to contributing to the further growth of nanowires and branching on their surface with a mechanism known as Oswald ripening [89].



**Figure 27** SEM images of Au nanostructures synthesized at different HMTA concentrations of (a) 0.03, (b) 0.05, (c) 0.1, (d) 0.3, and (e) 0.5 M.



**Figure 28** SEM images of Au nanostructures synthesized at different Na<sub>2</sub>-EDTA concentration of (a) 0.01, (b) 0.03, (c) 0.1, and (d) 0.3 M.

Change in concentration of Na<sub>2</sub>-EDTA was investigated in the range of 0.01 M - 0.3 M, while other parameters were kept constant. Figure 28 demonstrates SEM images of Au nanostructures synthesized at different concentrations of Na<sub>2</sub>-EDTA. Small, non-uniform, rod-like structures were formed when 0.01 M surfactant molecule was used as shown in Figure 28 (a). As the concentration was increased to 0.03 M, the welding or directional assembly of these short structures to form longer wires was observed (Figure 28 (b)). At 0.1 M and 0.3 M concentrations of Na<sub>2</sub>-EDTA, adhesion of nanowires and formation of micron-size structures were observed (Figure 28

(c) - (d)). The change in morphology of nanostructures with use of different surfactant molecules at high concentrations is presumable because of differences in their chelating properties as well as their electronic natures;  $\text{Na}_2\text{-EDTA}$  has anionic counterparts while HMTA is neutral. Figure 29 demonstrates the skeletal formula of  $\text{Na}_2\text{-EDTA}$  and HMTA.

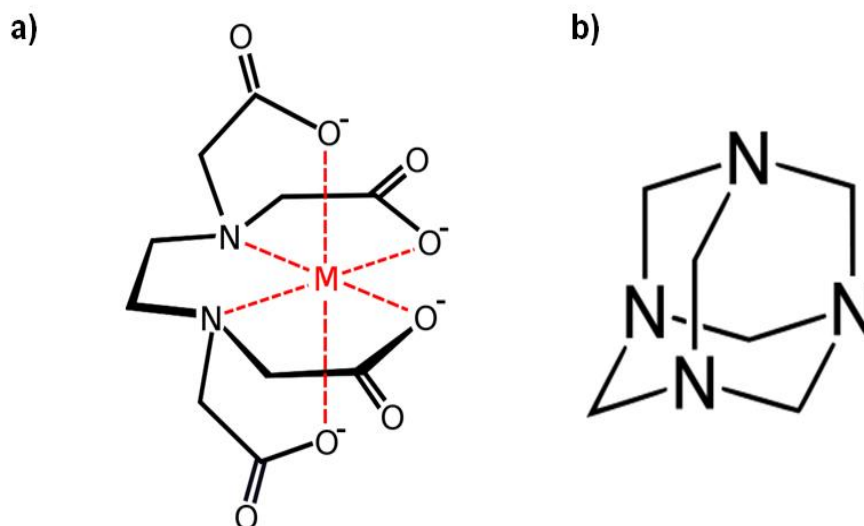


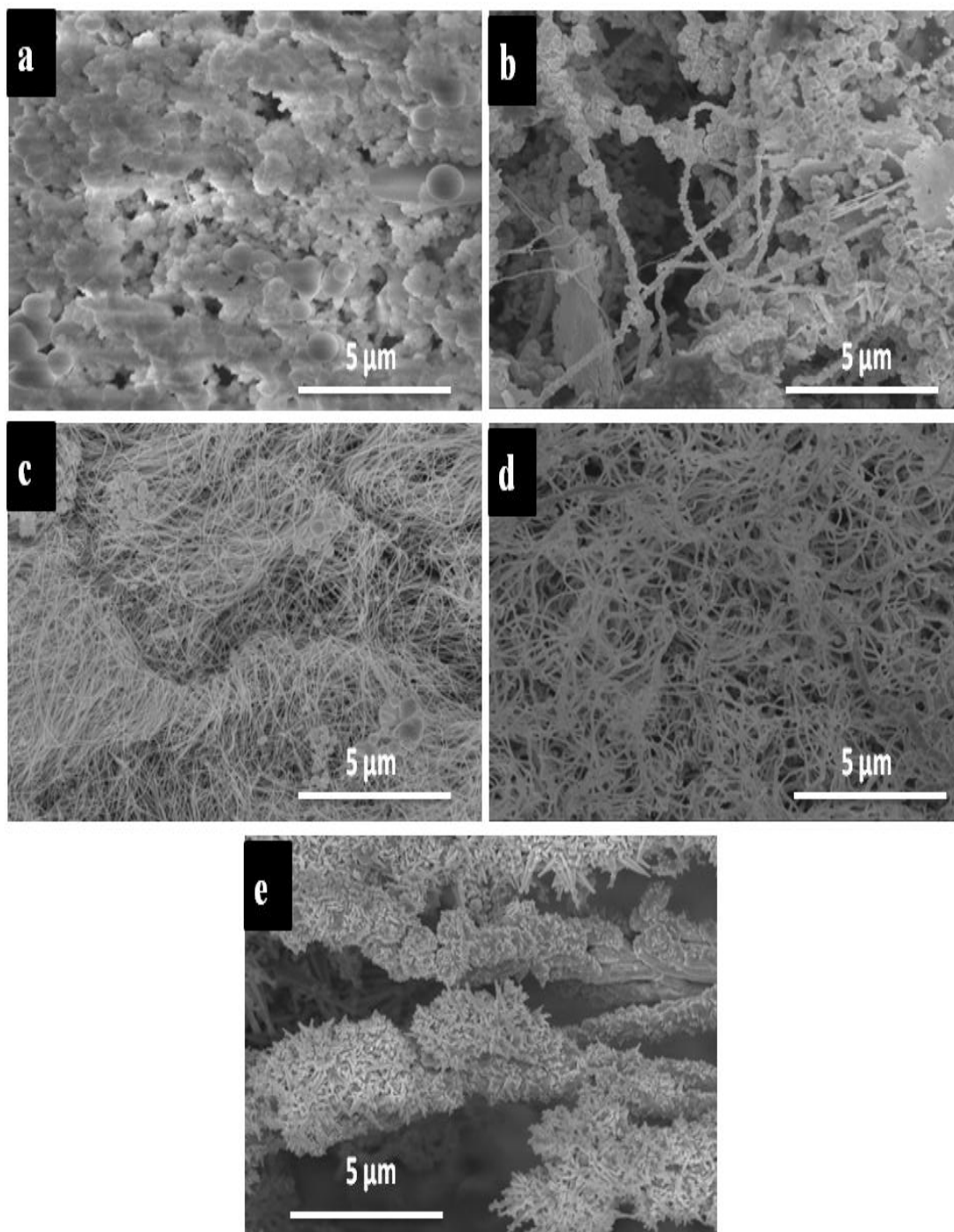
**Figure 29** Skeletal formulas of (a)  $\text{Na}_2\text{-EDTA}$  (b) HMTA.

#### 4.3.2 Effect of Temperature

Temperature of solution in MHT method is one of the other factor that has direct influence on morphology, structural purity and uniformity of the nanocrystals synthesized. Since the kinetic of reduction mechanism depends on the reaction temperature, purity, morphology, uniformity and thermal stability of Au nanowires can vary at different temperatures [88, 90]. Moreover, differences of vapor pressure and structure of water at elevated temperatures can affected properties (i.e. solubility, reactivity) of reactants and lead to formation of nanocrystals which cannot be obtained at room temperature [88, 90]. Crystallization, in general, is governed by two main factors: i) the degree of super saturation which has significant impact on the rate of nucleation and crystal growth, and ii) dynamic equilibrium of

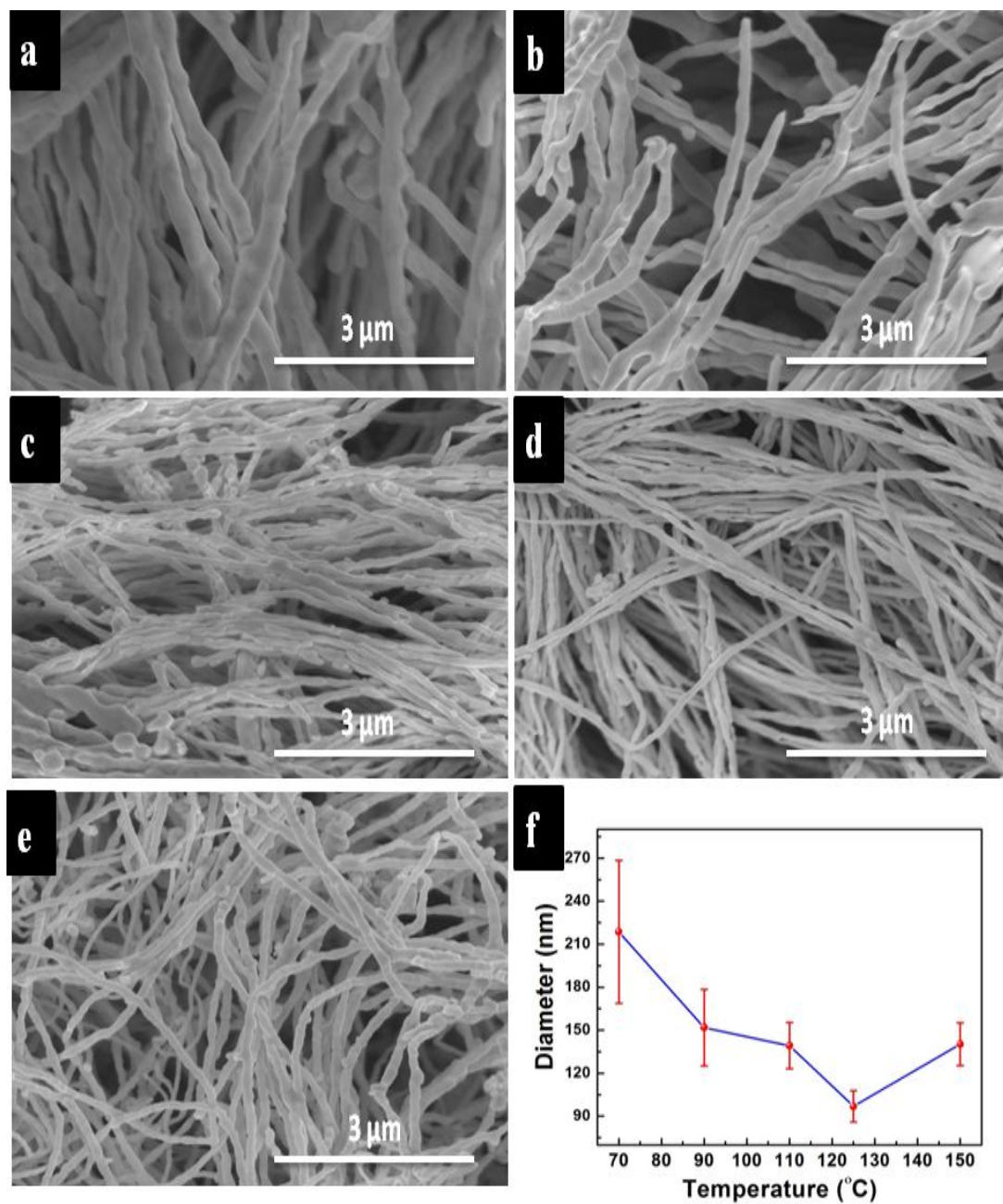
dissolution and crystallization processes [88, 90]. Manipulation of these kinetic and thermodynamic factors by temperature can lead to formation of desired crystals in hydrothermal process. In this study, different temperatures in the range of 70 °C -150 °C were investigated for both surfactant molecules (HMTA, Na<sub>2</sub>-EDTA). Also, increase in the quality (structural uniformity and purity) and yield of nanowires was observed with uniform heating which is obtained simply by keeping the reaction vessel in oil bath heated by a hot plate. This modification in the experimental set-up allowed us to control the temperature and study the temperature effect.

Figure 30 demonstrates the SEM images of nanostructures formed by using HMTA at temperatures between 70 °C and 150 °C. Nanowire formation was not obtained at 70 °C (Figure 30 (a)). When temperature was increased to 90 °C, non-uniform nanowires with very low yield started to form as shown in Figure 30 (b). Low rate of crystal growth along with high super saturation at this temperature are most likely reasons for the unwanted crystal growth. Significant increase in number of wires was observed as the temperature was increased to 110 °C (Figure 30 (c)). The nanowires have diameters in the range of 45 nm to 70 nm. Despite the formation of some nanocrystals with different morphologies, the highest yield and structural purity was obtained at this temperature. This suggests optimum kinetic and thermodynamic level was reached at 110 °C for growing desired nanocrystals. As the temperature increased to 125 °C, crystallization of nanostructures started earlier, and an increase in the diameter of nanowires (between 75 nm and 105 nm) was observed (Figure 30 (d) - (e)). Considerable structural change and formation of anisotropically grown micron size structures were observed upon further increase in the temperature to 150 °C (Figure 30 (e)). This is most likely due to disruption of dissolution-crystallization dynamic equilibrium by high dissolution rate at this temperature.



**Figure 30** SEM images of Au nanowires synthesized in the presence of HMTA at different temperatures (a) 70, (b) 90, (c) 110, (d) 125 and (e) 150 °C.

On the other hand, unlike HMTA, Au nanowires were obtained with all temperatures when Na<sub>2</sub>-EDTA was used as reducing and growth controlling agent (Figure 31 (a)-(e)). However, average diameters of Au nanowires vary significantly. The changes in nanowire diameter with reaction temperature are also shown in Figure 31 (f). Average diameter distribution is very broad at low temperatures; changing from 165 nm to 270 nm and from 120 nm to 180 nm range for 70 °C and 90 °C of reaction temperatures, respectively (Figure 31 (a)-(b)). Thickness of the nanowires decrease, and diameter distribution become narrower as the reaction temperature is increased (Figure 31 (c)). The smallest diameter and diameter distribution range were obtained when the reaction was carried out at 125 °C (Figure 31 (d)). Further increase in temperature to 150 °C results in increase both of these values (Figure 31 (e)), suggesting the optimum degree of super saturation and dynamic equilibrium were reached at 125 °C for the synthesis of nanowires with desired properties.



**Figure 31** SEM images of Au nanowires synthesized in the presence of Na<sub>2</sub>-EDTA at different temperatures (a) 70, (b) 90, (c) 110, (d) 125 and (e) 150 °C. (f) Changes in nanowire diameter with reaction temperature.

### 4.3.3 Effect of Reaction Time

Reaction time has a strong influence on the resultant nanowire morphology and structural purity. To investigate effect of this parameter, the experiments were conducted at 110 °C (for HMTA) and 125 °C (for Na<sub>2</sub>-EDTA) for 10 min, 30 min, 2 h, 4 h and 5 h. Figure 32 demonstrates SEM images of Au nanowires synthesized at 110 °C in the presence of HMTA within different reaction times. When HMTA was used as surfactant, only spherical nanoparticles were formed at the end of 10 minutes (Figure 32 (a)). Small nanoparticle formation with low thermodynamic stability occurs at early stages of reaction and they have tendency to grow into larger particles as a result of large free energy driving force [88]. When time was prolonged, nanowire formation started and increased for 30 minutes and 2 hours (Figure 32 (b)-(c)). However, purity of product was still very low and morphologies of nanowires were not uniform. The highest yield and structural purity was achieved when the reaction was carried out for 4 hours (Figure 32 (d)). At longer reaction times such as 5 hours, diameter of wires increases as well as their distribution (Figure 32 (e)). This is most likely due to decrease in the saturation degree as the reactants depleted. This initiate Ostwald ripening or defocusing and particles smaller than the critical nuclei size dissolve to contribute to the growth of larger particles.

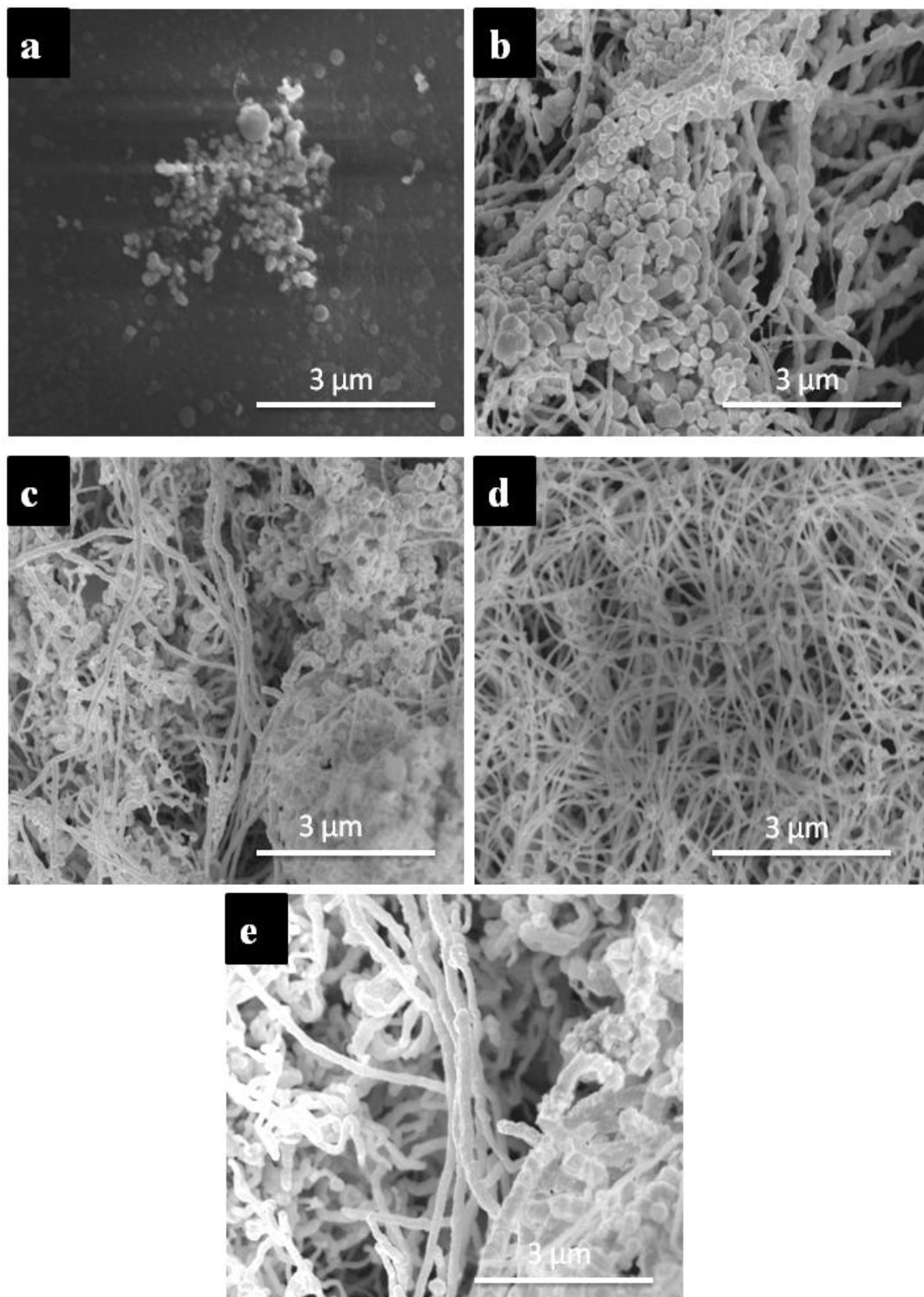


**Figure 32** SEM images of Au nanostructures synthesized in the presence of HMTA at 110 °C for (a) 10 min, (b) 30 min, (c) 2 hours, (d) 4 hours and (e) 5 hours.

The effect of reaction time was also investigated in the range of 10 min-5 hour, in the presence of Na<sub>2</sub>-EDTA. SEM images of the Au nanowires for 10 min, 30 min, 2 hours, 4 hours and 5 hours are shown in Figure 33 (a) - (f), respectively. Unlike HMTA, Au nanowires are observed just after 10 minutes (Figure 33 (a)). However, micron size structures were formed as well as nanowires during this period of time. After 2 hours, amount of by-product decreased but formation of Au nanowires could not be completed (Figure 33 (c)-(d)). Maximum yield and better morphology is provided when reaction was prolonged to 4 hours (Figure 33 (e)). Further extension of reaction time results in slight disruption of nanowire morphology and reformation of micron sized particles. As a result, the optimum time for the reactions carried out with both surfactant molecules is determined as 4 hours. The decrease in the reaction time for synthesis of high yield Au nanowires was observed compared to the one reported by Sinha et. al. [23] This is probably because of our modification in the experimental set-up providing temperature control and even heat distribution in the reaction vessel.

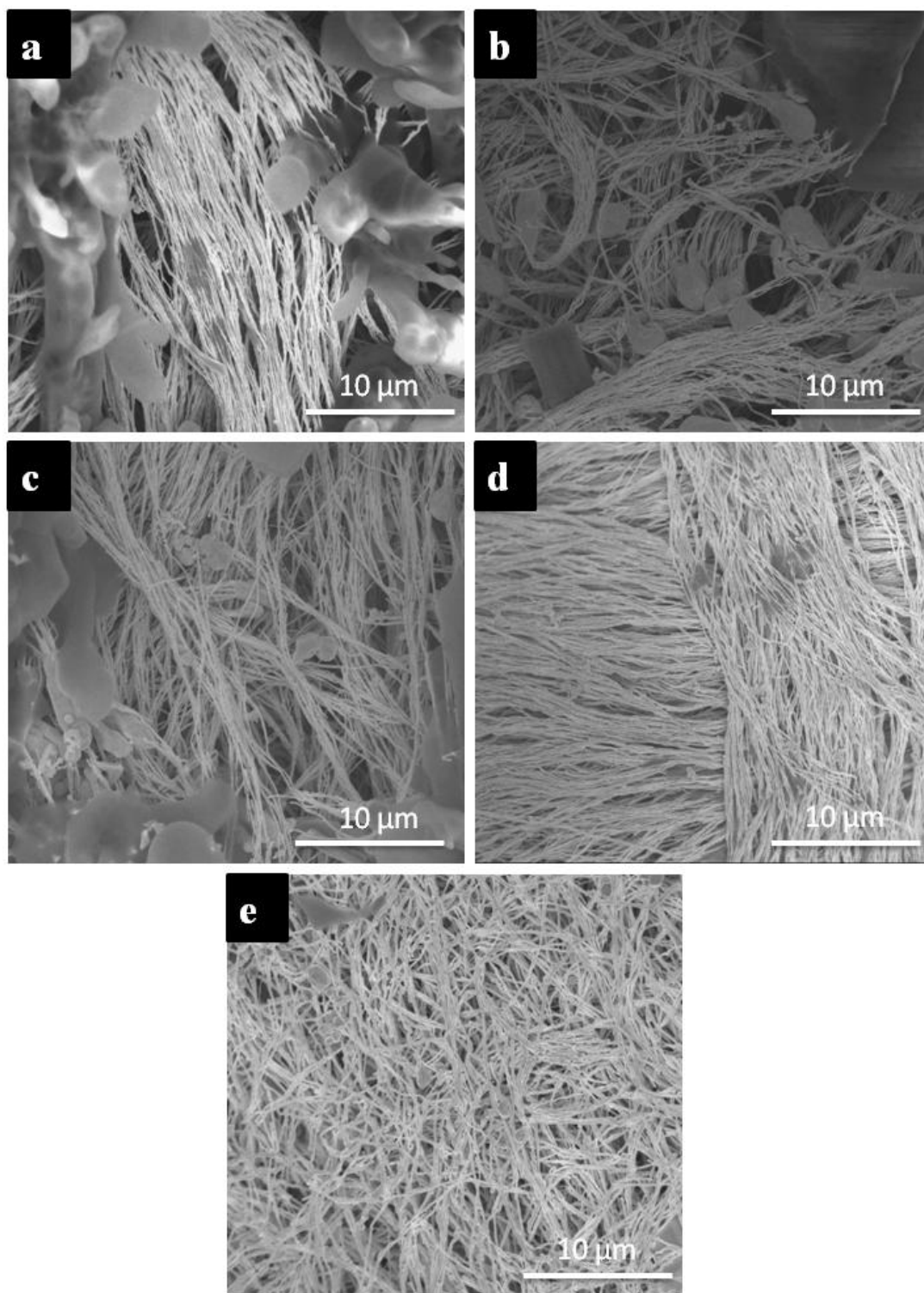


**Figure 33** SEM images of Au nanostructures synthesized in the presence of  $\text{Na}_2\text{-EDTA}$  at  $125\text{ }^\circ\text{C}$  for (a) 10 min, (b) 30 min, (c) 2 hours, (d) 4 hours and (e) 5 hours.

## CHAPTER 5

### CONCLUSIONS

The mechanism of modified hydrothermal process was investigated in detail. The process conditions for the synthesis of Au nanowires as a function of surfactant (HMTA and Na<sub>2</sub>-EDTA) concentration, reaction temperature and time was explored. For the first time, HMTA was used as a surfactant molecule for the synthesis of Au nanowires in addition to conventional Na<sub>2</sub>-EDTA. Optimum reaction conditions were determined for the synthesis of Au nanowires with high aspect ratio and structural purity for both surfactant molecules. Au nanowires with micrometer length and 50-110 nm radius was obtained at a concentration of 0.3 M, reaction time of 4 hours and reaction temperature at 110 °C for HMTA and 0.03 M concentration, reaction time of 4 hour and reaction temperature at 125 °C for Na<sub>2</sub>-EDTA. Higher yield of nanowires were obtained when Na<sub>2</sub>-EDTA was used. On the other hand, HMTA resulted in the formation of thinner nanowires with narrower diameter distribution compared to the ones synthesized in the presence of Na<sub>2</sub>-EDTA. Following the separation of Au nanowires they can be used in applications such as light emitting diodes, transparent conducting contacts (TCCs) and various others where enhanced optical properties or direct electrical conduction in nanoscale is needed.

## REFERENCES

- [1] K. J. Klabunde, R. Richards, and MyiLibrary, *Nanoscale materials in chemistry*, pp. 20-40: Wiley Online Library, 2001.
- [2] K. J. Klabunde *et al.*, "Nanocrystals as stoichiometric reagents with unique surface chemistry," *The Journal of Physical Chemistry*, vol. 100, no. 30, pp. 12142-12153, 1996.
- [3] J. García-Calzón, and M. E. Díaz-García, "Synthesis and analytical potential of silica nanotubes," *TrAC Trends in Analytical Chemistry*, 2012.
- [4] T. Sau, and C. Murphy, "Role of ions in the colloidal synthesis of gold nanowires," *Philosophical Magazine*, vol. 87, no. 14-15, pp. 2143-2158, 2007.
- [5] B. Bhushan, *Springer handbook of nanotechnology*: Springer Verlag, 2004.
- [6] Y. Yang *et al.*, "New nanostructured Li<sub>2</sub>S/silicon rechargeable battery with high specific energy," *Nano letters*, vol. 10, no. 4, pp. 1486-1491, 2010.
- [7] M. A. Zimmler *et al.*, "Electroluminescence from single nanowires by tunnel injection: an experimental study," *Nanotechnology*, vol. 18, pp. 235205, 2007.
- [8] Z. Wu *et al.*, "An all-inorganic type-II heterojunction array with nearly full solar spectral response based on ZnO/ZnSe core/shell nanowires," *J. Mater. Chem.*, vol. 21, no. 16, pp. 6020-6026, 2011.
- [9] K. Q Peng, Z. P Huang, and J. Zhu, "Fabrication of Large-Area Silicon Nanowire p-n Junction Diode Arrays," *Advanced Materials*, vol. 16, no. 1, pp. 73-76, 2004.
- [10] Y. Cui *et al.*, "High performance silicon nanowire field effect transistors," *Nano Letters*, vol. 3, no. 2, pp. 149-152, 2003.
- [11] A. B. Greytak *et al.*, "Growth and transport properties of complementary germanium nanowire field-effect transistors," *Applied Physics Letters*, vol. 84, pp. 4176, 2004.
- [12] F. Shen *et al.*, "Rapid Flu Diagnosis Using Silicon Nanowire Sensor," *Nano Letters*, 2012.
- [13] G. Shen *et al.*, "Devices and chemical sensing applications of metal oxide nanowires," *J. Mater. Chem.*, vol. 19, no. 7, pp. 828-839, 2009.
- [14] N. N. Greenwood, A. Earnshaw, and Knovel, "Chemistry of the Elements," 1984.
- [15] C. W. Kuo *et al.*, "Studies of Surface-Modified Gold Nanowires Inside Living Cells," *Advanced Functional Materials*, vol. 17, no. 18, pp. 3707-3714, 2007.

- [16] Z. Liu, and P. C. Searson, "Single nanoporous gold nanowire sensors," *The Journal of Physical Chemistry B*, vol. 110, no. 9, pp. 4318-4322, 2006.
- [17] <http://www.materials360online.com/newsDetails/10020> (10.08.2012)
- [18] <http://web.mit.edu/newsoffice/2011/gold-nanowire-heart-0926.html> (10.08.2012).
- [19] M. C. Rosamond *et al.*, "Transparent gold nanowire electrodes." pp. 604-607.
- [20] H. Lord, and S. O. Kelley, "Nanomaterials for ultrasensitive electrochemical nucleic acids biosensing," *Journal of Materials Chemistry*, vol. 19, no. 20, pp. 3127-3134, 2009.
- [21] Z. Zou, J. Kai, and C. H. Ahn, "Electrical characterization of suspended gold nanowire bridges with functionalized self-assembled monolayers using a top-down fabrication method," *Journal of Micromechanics and Microengineering*, vol. 19, pp. 055002, 2009.
- [22] B. D. Busbee, S. O. Obare, and C. J. Murphy, "An Improved Synthesis of High-Aspect-Ratio Gold Nanorods," *Advanced Materials*, vol. 15, no. 5, pp. 414-416, 2003.
- [23] A. K. Sinha *et al.*, "Electrostatic Field Force Directed Gold Nanowires from Anion Exchange Resin," *Langmuir*, 2010.
- [24] X. Huang, S. Neretina, and M. A. El-Sayed, "Gold nanorods: from synthesis and properties to biological and biomedical applications," *Advanced Materials*, vol. 21, no. 48, pp. 4880-4910, 2009.
- [25] L. Billot *et al.*, "Surface enhanced Raman scattering on gold nanowire arrays: Evidence of strong multipolar surface plasmon resonance enhancement," *Chemical physics letters*, vol. 422, no. 4, pp. 303-307, 2006.
- [26] W. S. Choi, T. An, and G. Lim, "Fabrication of Conducting Polymer Nanowires."
- [27] C. N. R. Rao, *The chemistry of nanomaterials: Synthesis, properties and applications*: Wiley-VCH, 2006.
- [28] J. Gu *et al.*, "A new strategy to incorporate high density gold nanowires into the channels of mesoporous silica thin films by electroless deposition," *Solid state sciences*, vol. 6, no. 7, pp. 747-752, 2004.
- [29] S. Karim *et al.*, "Synthesis of gold nanowires with controlled crystallographic characteristics," *Applied Physics A: Materials Science & Processing*, vol. 84, no. 4, pp. 403-407, 2006.
- [30] R. Köppe *et al.*, "Template-Fabricated Gold Nanowires from Gas-Phase Transport Reactions," *European journal of inorganic chemistry*, vol. 2005, no. 18, pp. 3657-3661, 2005.
- [31] R. M. Stoltenberg, and A. T. Woolley, "DNA-templated nanowire fabrication," *Biomedical microdevices*, vol. 6, no. 2, pp. 105-111, 2004.
- [32] A. Ongaro *et al.*, "DNA-templated assembly of conducting gold nanowires between gold electrodes on a silicon oxide substrate," *Chemistry of materials*, vol. 17, no. 8, pp. 1959-1964, 2005.
- [33] Y. Weizmann *et al.*, "Telomerase-generated templates for the growing of metal nanowires," *Nano Letters*, vol. 4, no. 5, pp. 787-792, 2004.

- [34] K. S. Shankar, and A. Raychaudhuri, "Fabrication of nanowires of multicomponent oxides: Review of recent advances," *Materials Science and Engineering: C*, vol. 25, no. 5, pp. 738-751, 2005.
- [35] E. Rossinyol *et al.*, "Nanostructured metal oxides synthesized by hard template method for gas sensing applications," *Sensors and Actuators B: Chemical*, vol. 109, no. 1, pp. 57-63, 2005.
- [36] C. Minelli *et al.*, "Micrometer-long gold nanowires fabricated using block copolymer templates," *Langmuir*, vol. 21, no. 16, pp. 7080-7082, 2005.
- [37] G. Kartopu, and O. Yalçın, "Fabrication and Applications of Metal Nanowire Arrays Electrodeposited in Ordered Porous Templates."
- [38] R. Dou, and B. Derby, "The strength of gold nanowire forests," *Scripta Materialia*, vol. 59, no. 2, pp. 151-154, 2008.
- [39] J. Liu *et al.*, "Electrochemical fabrication of single-crystalline and polycrystalline Au nanowires: the influence of deposition parameters," *Nanotechnology*, vol. 17, pp. 1922, 2006.
- [40] E. Walter *et al.*, "Noble and coinage metal nanowires by electrochemical step edge decoration," *The Journal of Physical Chemistry B*, vol. 106, no. 44, pp. 11407-11411, 2002.
- [41] S. A. Dong, and S. P. Zhou, "Photochemical synthesis of colloidal gold nanoparticles," *Materials Science and Engineering: B*, vol. 140, no. 3, pp. 153-159, 2007.
- [42] K. Esumi, K. Matsuhisa, and K. Torigoe, "Preparation of rodlike gold particles by UV irradiation using cationic micelles as a template," *Langmuir*, vol. 11, no. 9, pp. 3285-3287, 1995.
- [43] G. O. Mallory, and J. B. Hajdu, *Electroless plating: fundamentals and applications*: William Andrew, 1990.
- [44] G. Cao, and D. Liu, "Template-based synthesis of nanorod, nanowire, and nanotube arrays," *Advances in colloid and interface science*, vol. 136, no. 1-2, pp. 45-64, 2008.
- [45] H. Yao *et al.*, "Optical and electrical properties of gold nanowires synthesized by electrochemical deposition," *Journal of Applied Physics*, vol. 110, no. 9, pp. 094301-094301-6, 2011.
- [46] M. Wan, "A Template-Free Method Towards Conducting Polymer Nanostructures," *Advanced Materials*, vol. 20, no. 15, pp. 2926-2932, 2008.
- [47] J. Wiesner, and A. Wokaun, "Anisometric gold colloids. Preparation, characterization, and optical properties," *Chemical Physics Letters*, vol. 157, no. 6, pp. 569-575, 1989.
- [48] C. J. Murphy *et al.*, "Anisotropic metal nanoparticles: synthesis, assembly, and optical applications," *The Journal of Physical Chemistry B*, vol. 109, no. 29, pp. 13857-13870, 2005.
- [49] H. Y. Wu *et al.*, "Seed-mediated synthesis of high aspect ratio gold nanorods with nitric acid," *Chemistry of materials*, vol. 17, no. 25, pp. 6447-6451, 2005.
- [50] M. Iqbal, Y. I. Chung, and G. Tae, "An enhanced synthesis of gold nanorods by the addition of Pluronic (F-127) via a seed mediated growth process," *J. Mater. Chem.*, vol. 17, no. 4, pp. 335-342, 2007.

- [51] T. K. Sau, and C. J. Murphy, "Room temperature, high-yield synthesis of multiple shapes of gold nanoparticles in aqueous solution," *Journal of the American Chemical Society*, vol. 126, no. 28, pp. 8648-8649, 2004.
- [52] X. Kou *et al.*, "Growth of gold nanorods and bipyramids using CTEAB surfactant," *The Journal of Physical Chemistry B*, vol. 110, no. 33, pp. 16377-16383, 2006.
- [53] N. R. Jana, L. Gearheart, and C. Murphy, "Seed-mediated growth approach for shape-controlled synthesis of spheroidal and rod-like gold nanoparticles using a surfactant template," *Advanced Materials*, vol. 13, no. 18, pp. 1389-1393, 2001.
- [54] Y. Xia *et al.*, "Shape-Controlled Synthesis of Metal Nanocrystals: Simple Chemistry Meets Complex Physics," *Angewandte Chemie International Edition*, vol. 48, no. 1, pp. 60-103, 2009.
- [55] J. Xiao, and L. Qi, "Surfactant-assisted, shape-controlled synthesis of gold nanocrystals," *Nanoscale*, vol. 3, no. 4, pp. 1383-1396, 2011.
- [56] N. R. Jana, L. Gearheart, and C. J. Murphy, "Wet chemical synthesis of high aspect ratio cylindrical gold nanorods," *The Journal of Physical Chemistry B*, vol. 105, no. 19, pp. 4065-4067, 2001.
- [57] F. Kim *et al.*, "Chemical synthesis of gold nanowires in acidic solutions," *Journal of the American Chemical Society*, vol. 130, no. 44, pp. 14442-14443, 2008.
- [58] K. Byrappa, and T. Adschiri, "Hydrothermal technology for nanotechnology," *Progress in Crystal Growth and Characterization of Materials*, vol. 53, no. 2, pp. 117-166, 2007.
- [59] <http://nanotubes.epfl.ch/page-24503-en.html> (10.08.2012).
- [60] J. Yu *et al.*, "Effects of hydrothermal temperature and time on the photocatalytic activity and microstructures of bimodal mesoporous TiO<sub>2</sub> powders," *Applied Catalysis B: Environmental*, vol. 69, no. 3, pp. 171-180, 2007.
- [61] C. Y. Huang *et al.*, "The effects of hydrothermal temperature and thickness of TiO<sub>2</sub> film on the performance of a dye-sensitized solar cell," *Solar energy materials and solar cells*, vol. 90, no. 15, pp. 2391-2397, 2006.
- [62] C. H. Lu, and C. H. Yeh, "Influence of hydrothermal conditions on the morphology and particle size of zinc oxide powder," *Ceramics International*, vol. 26, no. 4, pp. 351-357, 2000.
- [63] K. Yanagisawa, and J. Ovenstone, "Crystallization of anatase from amorphous titania using the hydrothermal technique: effects of starting material and temperature," *The Journal of Physical Chemistry B*, vol. 103, no. 37, pp. 7781-7787, 1999.
- [64] H. Hayashi, and Y. Hakuta, "Hydrothermal Synthesis of Metal Oxide Nanoparticles in Supercritical Water," *Materials*, vol. 3, no. 7, pp. 3794-3817, 2010.
- [65] A. Elsanousi *et al.*, "Hydrothermal treatment duration effect on the transformation of titanate nanotubes into nanoribbons," *The Journal of Physical Chemistry C*, vol. 111, no. 39, pp. 14353-14357, 2007.

- [66] M. C. Akgun, Y. E. Kalay, and H. E. Unalan, "Hydrothermal zinc oxide nanowire growth using zinc acetate dihydrate salt," *Journal of Materials Research*, vol. 1, no. 1, pp. 1-7, 2012.
- [67] J. K. Han *et al.*, "Synthesis of high purity nano-sized hydroxyapatite powder by microwave-hydrothermal method," *Materials chemistry and physics*, vol. 99, no. 2, pp. 235-239, 2006.
- [68] J. Zhang, X. Xiao, and J. Nan, "Hydrothermal-hydrolysis synthesis and photocatalytic properties of nano-TiO<sub>2</sub> with an adjustable crystalline structure," *Journal of hazardous materials*, vol. 176, no. 1-3, pp. 617-622, 2010.
- [69] A. Tok *et al.*, "Hydrothermal synthesis of CeO<sub>2</sub> nano-particles," *Journal of materials processing technology*, vol. 190, no. 1, pp. 217-222, 2007.
- [70] Y. Ji *et al.*, "Single-crystalline SnS<sub>2</sub> nano-belts fabricated by a novel hydrothermal method," *Journal of Physics: Condensed Matter*, vol. 15, pp. L661, 2003.
- [71] C. Xiangfeng *et al.*, "Ethanol gas sensor based on CoFe<sub>2</sub>O<sub>4</sub> nano-crystallines prepared by hydrothermal method," *Sensors and Actuators B: Chemical*, vol. 120, no. 1, pp. 177-181, 2006.
- [72] M. Basu *et al.*, "Evolution of Hierarchical Hexagonal Stacked Plates of CuS from Liquid- Liquid Interface and its Photocatalytic Application for Oxidative Degradation of Different Dyes under Indoor Lighting," *Environmental science & technology*, 2010.
- [73] A. K. Sinha *et al.*, "Fabrication of Large-Scale Hierarchical ZnO Hollow Spheroids for Hydrophobicity and Photocatalysis," *Chemistry-A European Journal*, vol. 16, no. 26, pp. 7865-7874, 2010.
- [74] M. Basu *et al.*, "Hierarchical Superparamagnetic Magnetite Nanowafers from a Resin-Bound [Fe (bpy) 3] 2+ Matrix," *Langmuir*, vol. 26, no. 8, pp. 5836-5842, 2009.
- [75] A. K. Sinha *et al.*, "New hydrothermal process for hierarchical TiO<sub>2</sub> nanostructures," *CrystEngComm*, vol. 11, no. 7, pp. 1210-1212, 2009.
- [76] Z. L. Wang, "ZnO nanowire and nanobelt platform for nanotechnology," *Materials Science and Engineering: R: Reports*, vol. 64, no. 3-4, pp. 33-71, 2009.
- [77] A. Ismail *et al.*, "Application of statistical design to optimize the preparation of ZnO nanoparticles via hydrothermal technique," *Materials Letters*, vol. 59, no. 14, pp. 1924-1928, 2005.
- [78] S. H. Ko *et al.*, "Nanoforest of hydrothermally grown hierarchical ZnO nanowires for a high efficiency dye-sensitized solar cell," *Nano letters*, 2011.
- [79] R. Savu *et al.*, "The effect of cooling rate during hydrothermal synthesis of ZnO nanorods," *Journal of Crystal Growth*, vol. 311, no. 16, pp. 4102-4108, 2009.
- [80] J. Hu *et al.*, "One-step synthesis of graphene-AuNPs by HMTA and the electrocatalytical application for O<sub>2</sub> and H<sub>2</sub>O<sub>2</sub>," *Talanta*, 2012.
- [81] A. Ali Umar, and M. Oyama, "High-Yield Synthesis of Tetrahedral-Like Gold Nanotripods Using an Aqueous Binary Mixture of Cetyltrimethylammonium Bromide and Hexamethylenetetramine," *Crystal Growth and Design*, vol. 9, no. 2, pp. 1146-1152, 2008.

- [82] C. Li *et al.*, "Electrochemical acetylene sensor based on Au/MWCNTs," *Sensors and Actuators B: Chemical*, vol. 149, no. 2, pp. 427-431, 2010.
- [83] H. T. Zhang *et al.*, "Engineering magnetic properties of Ni nanoparticles by non-magnetic cores," *Chemistry of Materials*, vol. 21, no. 21, pp. 5222-5228, 2009.
- [84] G. Lü *et al.*, "Gold nanoparticles in mesoporous materials showing catalytic selective oxidation cyclohexane using oxygen," *Applied Catalysis A: General*, vol. 280, no. 2, pp. 175-180, 2005.
- [85] R. L. Whetten *et al.*, "Nanocrystal gold molecules," *Advanced materials*, vol. 8, no. 5, pp. 428-433, 1996.
- [86] C. H. Kuo, and M. H. Huang, "Synthesis of branched gold nanocrystals by a seeding growth approach," *Langmuir*, vol. 21, no. 5, pp. 2012-2016, 2005.
- [87] X. Zhang *et al.*, "Fabrication and characterization of highly ordered Au nanowire arrays," *Journal of Materials Chemistry*, vol. 11, no. 6, pp. 1732-1734, 2001.
- [88] C. Burda *et al.*, "Chemistry and properties of nanocrystals of different shapes," *Chemical Reviews-Columbus*, vol. 105, no. 4, pp. 1025-1102, 2005.
- [89] L. Pei, K. Mori, and M. Adachi, "Formation process of two-dimensional networked gold nanowires by citrate reduction of AuCl<sub>4</sub>-and the shape stabilization," *Langmuir*, vol. 20, no. 18, pp. 7837-7843, 2004.
- [90] P. Knauth, and J. Schoonman, *Nanostructured materials: selected synthesis methods, properties, and applications*: Kluwer Academic Pub, 2002.